

Designing the Optimal Bit: Balancing Energetic Cost, Speed and Reliability

Abhishek Deshpande^{1,2}, Manoj Gopalkrishnan³, Thomas E. Ouldridge⁴, and Nick S. Jones¹

¹*Department of Mathematics, Imperial College London, London SW7 2AZ, United Kingdom*

²*School of Technology and Computer Science, Tata Institute of Fundamental Research, Mumbai 400005, India*

³*Department of Electrical Engineering, Indian Institute of Technology Bombay, Mumbai 400076, India*

⁴*Department of Bioengineering, Imperial College London, London SW7 2AZ, United Kingdom*

Abstract

We consider the technologically relevant costs of operating a reliable bit that can be erased rapidly. We find that both erasing and reliability times are non-monotonic in the underlying friction, leading to a trade-off between erasing speed and bit reliability. Fast erasure is possible at the expense of low reliability at moderate friction, and high reliability comes at the expense of slow erasure in the underdamped and overdamped limits. Within a given class of bit parameters and control strategies, we define “optimal” designs of bits that meet the desired reliability and erasing time requirements with the lowest operational work cost. We find that optimal designs always saturate the bound on the erasing time requirement, but can exceed the required reliability time if critically damped. The non-trivial geometry of the reliability and erasing time-scales allows us to exclude large regions of parameter space as suboptimal. We find that optimal designs are either critically damped or close to critical damping under the erasing procedure.

Keywords: erasing/switching a bit, particle in a double well, reliability of information, optimal bit, friction trade-off, saturation/unsaturation of time-scales

1 Introduction

Certain information processing operations require work input. For example, Szilard and others [44, 24, 6, 7, 8] showed that erasing a bit requires at least $k_B T \log 2$ units of external work. This limit is a lower bound. In practice, devices spend many orders of magnitude more than this for erasing a bit [12, 32]. Insights gained from thinking about the lower bound have not yet translated into more energy-efficient technology.

We ask: given practical considerations like speed of operation, length-scale for device fabrication and operation, difficulties with energy recovery, and limitations in the design parameters considered, how would one go about designing information processing operations to operate as close to minimal energy requirements as possible? Is there a “Goldilocks zone” in the space of design parameters particularly suited to the operation of bits?

This question has obvious technological relevance in the context of low power computing [39, 38, 34]. It is also of independent scientific relevance in the context of living systems. Since the discovery of the structure of DNA and the central dogma of molecular biology, it has become well accepted that information processing is at the heart of many natural phenomena. Biological information processing is also limited by considerations of energy, as well as other considerations like speed, length scale, and reliability [6, 46, 23, 16, 28, 10, 5].

We consider a paradigmatic model of a bit as a particle in a 1-D potential, which is a quartic double-well potential in the device’s “resting” state. We require that the bit be reliable, so that a particle equilibrated in either well stays in that well for a specified long time on average. Simultaneously, we require the implementation of an “erase” or “reset” operation using an external control, so that erasure is completed within a specified short amount of time. Our principal question is to find values for the design parameters which consist of the height of the double well, the friction coefficient, and the control parameters to guarantee these requirements without expending more energy than required. Our principal contribution is an exploration of this design space, and a demarcation of a “Goldilocks zone” where the friction coefficient takes moderate values. This is somewhat counter-intuitive because historically friction has been viewed as a nuisance to computing, to be sent as low as possible [2, 11, 20, 25].

In Section 2, we describe the model of a bit on which we base all our subsequent analysis. We formalize the time-scale for which the bit stores information through the notion of **reliability time**. In Section 2.2.1, we describe one simple family of control protocols for resetting a bit. We calculate the work done in erasing a bit for this form of control. We will use this particular control protocol to illustrate our subsequent ideas. In Section 2.2.2, we introduce the notion of **erasing time**. In Section 3, we consolidate from the literature the analytical forms and approximations for our two time-scales of interest, and confirm them with numerical simulations. We find that both the reliability and erasing time-scales are non-monotonic, roughly U-shaped functions of the friction coefficient. It follows that high reliability is obtained by setting the friction to a low or high value, whereas a low erasing time is favoured by an intermediate value of friction. In Section 4, we investigate the geometry of **optimal bits**: bits that fulfil the desired reliability and erasing time requirements with the minimum energy cost. We find and partially characterize a “Goldilocks zone” in design space where optimal bits reside. In Section 5, we discuss the robustness of our results when more freedom is allowed in the choice of design parameters, and the control protocol.

2 The Double-Well Bit

We will represent a device to store one bit of information by a particle in a symmetric bistable potential $U_{A,B}(x) = A \left(\frac{x^2}{B^2} - 1 \right)^2$, where A is the height of the well and $\pm B$ are the coordinates of the minima of the right and left wells. We will refer to the device as a whole by “a bit”. The device reports “0” when the particle is in the left well, i.e., $x < 0$ and reports “1” otherwise (Figure 1a).

The dynamics of the particle is described by the Langevin equation.

$$\begin{aligned} m dx &= p dt \\ dp &= -\gamma p dt - \partial_x U_{A,B}(x) dt + \sqrt{2m\gamma k_B T} dW \end{aligned} \tag{1}$$

where m is the mass of the particle, x is position, p is momentum, γ is the friction coefficient of the medium, $U_{A,B}(x)$ is the potential, k_B is Boltzmann’s constant, and T is the

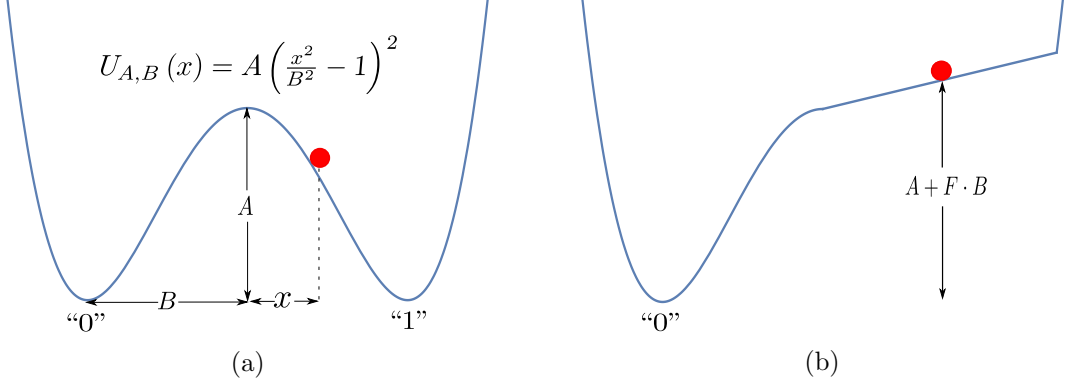


FIGURE 1: A bit as represented by a particle in a 1-D potential. Figure 1a: the bit in its resting state, with a barrier of height “A” separating particle locations that correspond to bit values of 0 or 1. Figure 1b: a control potential as in Example 2.1 is applied to erase the stored data.

temperature of the heat bath. The term $\sqrt{2m\gamma k_B T} dW$ represents the effect of noise from the surroundings. The Langevin equation is a stochastic differential equation, to be mathematically interpreted as a Stratonovich integral. For our case both the Ito and Stratonovich interpretations coincide [21, pp. 109] since the noise coefficient $\sqrt{2m\gamma k_B T}$ does not depend upon p .

From [29, pp. 182], the generator for the Langevin equation 1 is

$$\mathcal{L} = \frac{p}{m} \partial_x - (\partial_x U_{A,B}(x)) \partial_p + \gamma (-p \partial_p + k_B T \partial_p^2) \quad (2)$$

The **Hamiltonian** of the system is $H(x, p) = U_{A,B}(x) + \frac{p^2}{2m}$. The **Gibbs distribution**

$$\pi(x, p) = \frac{e^{-H(x, p)/k_B T}}{\int_{-\infty}^{\infty} \int_{-\infty}^{\infty} e^{-H(x', p')/k_B T} dx' dp'} \quad (3)$$

is approached as the system relaxes to equilibrium. Convergence to $\pi(x, p)$ happens exponentially fast at a rate given by the first non-zero eigenvalue of the generator \mathcal{L} [26].

2.1 Reliability

A device to store information should be able to store it with high fidelity for a specified long period of time. We introduce the **reliability time** to represent the time-scale over which our device can store data. Specifically, we define the reliability time τ_r as the expected first passage time for the particle to cross the barrier of the resting-state potential of the bit, given the Gibbs distribution $\pi(x, p)$ (Equation 3) as the initial distribution. That is,

$$\tau_r := \mathbb{E} [\inf\{t \geq 0 \mid x(t) = 0\}] \quad (4)$$

where the expectation is over trajectories $(x(t), p(t))$ distributed as specified by Equation 1 from the initial condition $(x(0), p(0)) \sim_{\text{law}} \pi(x, p)$. Note that τ_r is also the first passage time to cross the barrier for a bit prepared with a Gibbs distribution, but confined to either

the left-hand well $\pi_0(x, p)$ or right-hand well $\pi_1(x, p)$.

$$\pi_0(x, p) = \begin{cases} 2\pi(x, p) & \text{if } x < 0 \\ 0 & \text{otherwise} \end{cases}, \quad \pi_1(x, p) = \begin{cases} 2\pi(x, p) & \text{if } x > 0 \\ 0 & \text{otherwise} \end{cases}. \quad (5)$$

Intuitively, once a typical particle has had enough time to reach the top of the barrier, the data stored is no longer reliable.

2.2 Setting information

A device intended to store information must provide functionality to load, or set this information into the device. Setting information is a two-bit operation. A common use case is when a reference bit and the bit to be set are initially at some arbitrary values. We require that after the SET operation the reference bit is unchanged whereas the bit to be set now holds a copy of the reference bit. This is the operation that Szilard [44] refers to as “copying” (in contrast, Landauer [24, 14] chooses to reserve the word “copying” for the operation where the bit to be set is initially already known to be in the state “0”).

Note that in the operation of setting information, or copying in the sense of Szilard, initially the two bits are uncorrelated and unknown whereas after the operation they are still unknown but correlated. Thus implementing this operation requires decreasing the entropy of the system. Since it is easier to study a one-bit system rather than a two-bit system, we will investigate a one-bit proxy for the task of decreasing the entropy of the system, which is the task of **erasing** a bit.

Erasing involves taking a device whose initial state is maximally unknown into a known reference state, usually “0.” Somewhat counter intuitively, given the name, erasing increases the information we know about the system. What is erased is not information but randomness. It helps to keep in mind the example of erasing a blackboard where some random state with chalk marks is reset to the “all clear” state.

2.2.1 Erasing

The example that follows describes a simple family of control potentials to implement the erasing operation for our device, which will form the basis of our analysis. One control potential from this family is illustrated in Figure 1b. We chose such a simple class of controls to make a full understanding feasible, setting a framework for analysing more complex protocols. We also note that arbitrary variation of a physical potential in reality is highly non-trivial; experimental studies in which complex time-dependent potentials have been applied in fact use highly dissipate mechanisms to generate “effective” potentials [9, 19].

Example 2.1. Our control potentials are described by a single parameter $F \in \mathbb{R}_{>0}$ as follows.

$$V_F(x) := \begin{cases} A + F \cdot x - U_{A,B}(x) & \text{if } x \geq 0 \text{ and } A - U_{A,B}(x) + F \cdot x \geq 0, \\ 0 & \text{otherwise.} \end{cases} \quad (6)$$

The Langevin equation in the presence of control is

$$\begin{aligned} m dx &= p dt \\ dp &= -\gamma p dt - \partial_x U_{A,B}(x) dt - \partial_x V_F(x) dt + \sqrt{2m\gamma k_B T} dW \end{aligned} \quad (7)$$

Note that the control potential, as defined, is not differentiable at the boundary of the region in which it is non-zero. In practice, we assume that $\partial_x V_F$ changes rapidly but continuously in a small vicinity around these points.

In this work, we will consider variation of A , F and γ at fixed m , B , and T . In this case, m specifies the natural mass scale, B the natural length scale and $k_B T$ the natural energy scale; the natural time scale is then $\sqrt{mB^2/k_B T}$. Henceforth, all numerical quantities will be reported using reduced units defined with respect to these natural scales, although m , B and $k_B T$ will be retained within formulae.

2.2.2 Operational view of Erasing

The speed of bit operations is of practical importance: a useful bit must be reliable on much larger time-scales than those required to set or switch it. The control is switched on at time 0 and switched off at an appropriately-chosen time τ . The time τ is chosen beforehand, and does not depend on details of individual trajectories – a trajectory-dependent control would require measurement and feedback that itself would need accounting for [37, 36, 31, 1, 18, 43]. We could declare erasing as completed and switch off the control as soon as a majority of trajectories are expected to be in the left well. However, many of these “erased” bits would have high energies compared to typical bits drawn from the equilibrium distribution in the left well, $\pi_0(x, p)$. Thus they could rapidly return to the right well after a very short stay in the left well. So we insist on a more stringent condition. We require that the time τ should be large enough so that the majority of bits are in the target well, with an expected next passage time close to the reliability time.

One way to guarantee that the next passage time is high is by insisting on mixing, in the sense that the initial distribution $\pi(x, p)$ comes close to a distribution of particles thermalised in the left-hand well, $\pi_0(x, p)$. If this happens, we can guarantee that the expected next passage time will be equal to, or close to, the expected first passage time. However, we found this criterion too stringent for the following reason. At the end of the erasing protocol, it is not necessary that the distribution is close to $\pi_0(x, p)$ – only that the particles tend to relax to this distribution much faster than they cross back into the right-hand well, and thus have barrier passage times representative of particles initialised with $\pi_0(x, p)$.

Instead we proceed as follows. We define an **erasure region** in well “0” as all points (x, p) with total energy $H(x, p) \leq A - 3k_B T$ where A is the barrier height. We look for the time required for majority of the particles to reach the erasure region. The $3k_B T$ criterion has been used before by Vega et al. [47] to study atom-surface diffusion. It has the merit that it provides a clear computable criterion for erasing. We now argue that this definition is a good proxy for the criterion of reaching a state with an expected next passage time close to the reliability time.

For a range of well parameters, we used the Langevin A algorithm from [35] (refer to Section A of the Appendix for integrator set-up and validation), to estimate $\tau(x, p)$, the average barrier crossing time for particles initialised at position x with momentum p in the left well, for a grid of points (x, p) . The average reliability time for a given well can be

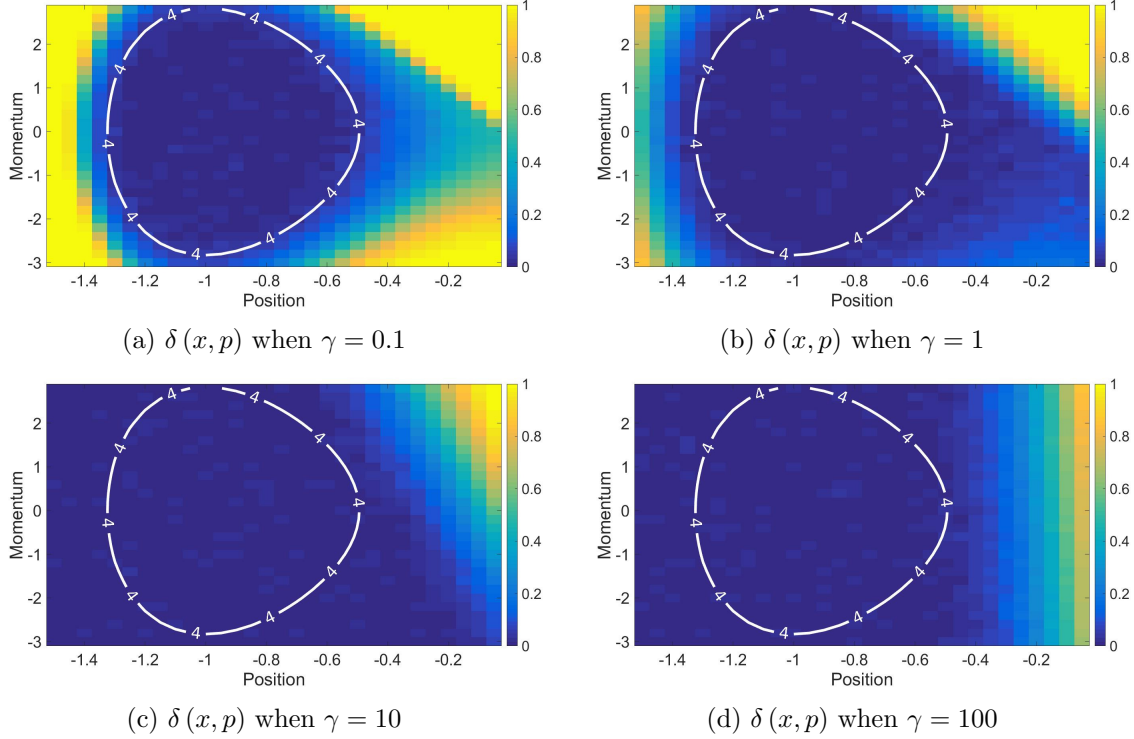


FIGURE 2: For particles initiated with $H(x, p) \leq A - 3k_B T$, well escape times are close to τ_r . Heat maps show the fractional deviation in expected escape time from the well-thermalised average τ_r , as a function of initial position and momentum, $\delta(x, p)$. The labelled contours correspond to a well height $A = 7$ with energy $H(x, p) = A - 3k_B T = 4k_B T$. These heat maps are representative of the situation for other barrier heights $A \geq 5k_B T$.

approximated in terms of $\tau(x, p)$ as follows:

$$\tau_r \approx \frac{\sum_{x,p} \tau(x, p) e^{-H(x,p)/k_B T}}{\sum_{x,p} e^{-H(x,p)/k_B T}}. \quad (8)$$

The deviation $\delta(x, p) := |1 - \frac{\tau(x,p)}{\tau_r}|$ for every point (x, p) in the grid is plotted in Figure 2, for a range of friction parameters at well height $A = 7$. It is clear that, for all values of friction, the points with total energy $H(x, p) \leq A - 3k_B T$ have reliability times close to τ_r . The same is true of other well heights A . This is because such particles typically undergo thermal mixing before they can escape the well. Once mixed, their next escape over the barrier will be on a time-scale of the order of τ_r .

Despite the robustness of this result to the value of the friction, the heatmaps in Figure 2 are friction-dependent. When γ is low, the particle diffuses very slowly in energy space, and it is the challenge of diffusing within this energy space that prohibits escape from the well. As a result the heatmap corresponding to $\gamma = 0.1$ (Figure 2a) follows the shape of constant energy contours. As friction starts increasing (e.g. in Figure 2b and 2c), diffusion in momentum-space becomes more rapid, but diffusion in position-space slows down. Once γ becomes very

high (e.g. $\gamma = 100$ in Figure 2d), the behaviour of the heatmap is essentially determined by the initial position of the particle; those close to the barrier and with $U_{A,B}(x)$ sufficiently close to A can escape easily, but the momentum is irrelevant. Using the total energy $H(x, p)$ as a criterion ensures that we account for all the regimes of friction.

Since we are interested in the typical time scale of transferring particles to a different well from the existent well, we will sample initial points only from the right well. We define the **erasing time** τ_e as the expected time to hit the erasure region, given that the particle started in the right-hand well:

$$\tau_e = \mathbb{E} [\inf\{t \geq 0 \mid x(t) < 0 \text{ and } H(x(t), p(t)) \leq A - 3k_B T\}] \quad (9)$$

where $(x(t), p(t))$ is the solution to Equation 7 with the initial condition $(x(0), p(0)) \sim_{\text{law}} \pi_1(x, p)$. Given this definition, τ_e indicates a typical time scale over which the control must be applied to successfully erase a large fraction of the bits. In practice, the control would be applied for a period $\tau > \tau_e$ to achieve high accuracy. We will use τ_e as an indicative time scale of control operation for the purposes of our analysis.

It is useful to decompose the erasing time τ_e as the sum of two times: the **transport time** and **mixing time**.

- **Transport time** (τ_t): The time taken by the particle to reach well “0” given that it is initially distributed according to $\pi_1(x, p)$.

$$\tau_t = \mathbb{E} [\inf\{t \geq 0 \mid x(t) \leq 0\}] \quad (10)$$

where $x(t)$ is the solution to Equation 7 with the initial condition $(x(0), p(0)) \sim_{\text{law}} \pi_1(x, p)$.

- **Mixing time** (τ_m): The time taken by the particle to mix sufficiently inside the well. This is the time starting from when the particle first reaches well “0” to when it first hits the erasure region.

$$\tau_m = \tau_e - \tau_t \quad (11)$$

2.2.3 Cost of erasing

In this section, we calculate the work done in erasing a bit. From Sekimoto’s expression [41, 42], for a protocol applied for a time τ and with a region of effect $I = \{x \geq 0 \mid A - U_{A,B}(x) + F \cdot x \geq 0\}$,

$$\langle W \rangle := \int_0^\tau \int_{x \in I} \frac{\partial V_F(x, t)}{\partial t} p(x, t) dx dt, \quad (12)$$

where $p(x, t)dxdt$ is the probability that the particle is between position $(x, x+dx)$ in the time interval $(t, t+dt)$. There are two potential sources of work that appear in our calculation.

1. When we begin the erasure protocol by switching on the control to lift the particle.
2. At the end of the protocol when we switch off the control.

We note that in our family of controls, there is negligible energy recovered when the control is switched off (refer to Section B.2 of the Appendix), since the probability of the particle being in the region in which the control is applied is small. More generally, the question of whether energy might be recovered from small systems and stored efficiently is a complex one, despite the optimism shown in previous discussions of erasing. Indeed, current technology does not attempt to recover any energy from bits.

We now calculate the work done for our protocol, Example 2.1. The particle's initial potential energy is approximately $k_B T/2$ on average, due to the equipartition theorem, and after the control is switched the average potential energy is $A + F \cdot B$ for a particle in the right well, since the particle is localised around $x = B$, and still $k_B T/2$ for a particle in the left well. So, ignoring energy recovery at the end of the operation, the net work done for the erasure protocol is $W = (A + F \cdot B - k_B T/2)/2$. As justified analytically and numerically in Section B.1 of the Appendix, this approximation is accurate for the values of A and F that we consider, and we will use this as the form of work for the rest of the manuscript.

Observation 2.2. Work is an increasing function of well height A at fixed F and γ . This follows immediately from the expression of work $W = (A + F \cdot B - k_B T/2)/2$.

3 Friction-based trade-offs for reliability and erasing

We explore the behaviour of the reliability and erasing time-scales as functions of the friction coefficient. We find that both these time-scales are non-monotonic, roughly U-shaped functions of the friction coefficient. A high reliability time requirement is favoured by a very low or very high friction; whereas a low erasing time requirement is helped by the choice of a moderate value of friction. Since a bit designer would seek reliable bits (needing high or low friction) that can be erased fast (needing intermediate friction), this yields a friction-based trade-off between reliability and speed of erasure. We explain this effect using the example control 2.1 for erasing a bit.

3.1 Reliability Time

Our definition of reliability time (Equation 4) is very similar to the classic problem of escape rates from one-dimensional wells (Fig 3), as applied in transition state theory to understand chemical reactions. In a famous paper [22], Kramer found analytic expressions for the escape rate k from a well by calculating the flux of particles between a source on one side of the barrier (x_A) and a sink at the other side (x_B). Kramer's expressions apply separately to the regimes of low friction, moderate to high friction and very high friction. Later the groups of Melnikov and Meshkov [27] and Pollack, Grabert and Hänggi [30] gave formulae that interpolate accurately over all values of friction (see review in [17]). We will apply the result of Melnikov and Meshkov to estimate analytical forms of the escape rate for our bistable system

$$k = \frac{\omega_0}{2\pi} \left[\sqrt{1 + \frac{\gamma^2}{4\omega_b^2}} - \frac{\gamma}{2\omega_b} \right] g e^{-A/k_B T}, \text{ where} \quad (13)$$

$$\log g = \frac{1}{2\pi} \int_0^{\frac{\pi}{2}} \log \left[1 - \exp \left(\frac{-\gamma I(A)}{4k_B T \cos^2 x} \right) \right] dx.$$

Here, ω_b is the angular frequency at barrier height, ω_0 is the angular frequency at the bottom of the well and $I(A)$ is the action for barrier height A . Refer to Section D in the Appendix for a detailed definition of these parameters and calculations for our system.

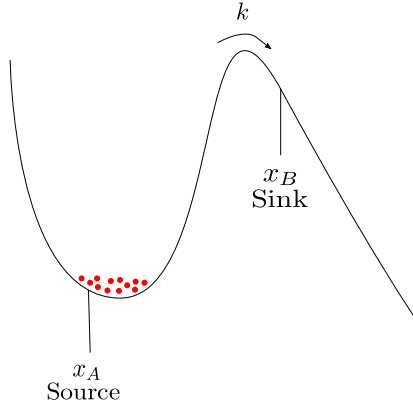


FIGURE 3: The escape of particles from a one-dimensional well. Kramer [22] considered a source of particles at the bottom of the well, and estimated the rate of escape to a sink on the far side of a barrier.

We plot the analytical prediction of $1/k$ given by Eq. 13 in Fig. 4 for two values of well height A , as a function of friction γ . This prediction is compared to average first passage time for particles to reach the top of the barrier from an initial Boltzmann distribution within a single well. The two quantities differ at large γ because Kramer's definition does not treat a particle that crosses the barrier but then immediately crosses back as having "escaped", whereas our definition of reliability in terms of a first passage time treats such particles as no longer being reliable. In the underdamped regime, immediate recrossings are rare and hence τ_r and $1/k$ coincide; in the overdamped regime, particles that reach the barrier top have a 50% chance of returning and so $\tau_r = 1/2k$. As can be seen from Fig. 4, τ_r smoothly interpolates between $\frac{1}{k}$ and $\frac{1}{2k}$, with the small numerical factor providing only a minor correction to the underlying physics of the analytical expression in Eq. 13.

The Melnikov-Meshkov expression predicts an almost-exponential scaling of $1/k$ with barrier height A , which is reproduced by τ_r and expected from the Arrhenius rate law [3]. Note that both $1/k$ and τ_r are non-monotonic in friction γ , with long reliability times in the underdamped and overdamped limits. This behaviour results from the need for particles to diffuse in both position and energy in order to reach the top of the barrier from an initial state thermalized within a single well. At high friction, particles rapidly sample different kinetic energies due to strong coupling with the environment, but move slowly in position space and hence take a long time to cross the barrier. At low friction, particles can move rapidly but their energy remains effectively constant over short time periods. They only cross the barrier when they have eventually gained enough total energy. Intermediate friction, when neither process is excessively slow, gives the shortest τ_r . This behaviour is typical of equilibrating systems in which an initial out-of-equilibrium condition (particles are guaranteed to be on one side of the well and not the other) relaxes towards an equilibrium state (particles on both sides of the barrier), and is thus insensitive to the details of our bit design.

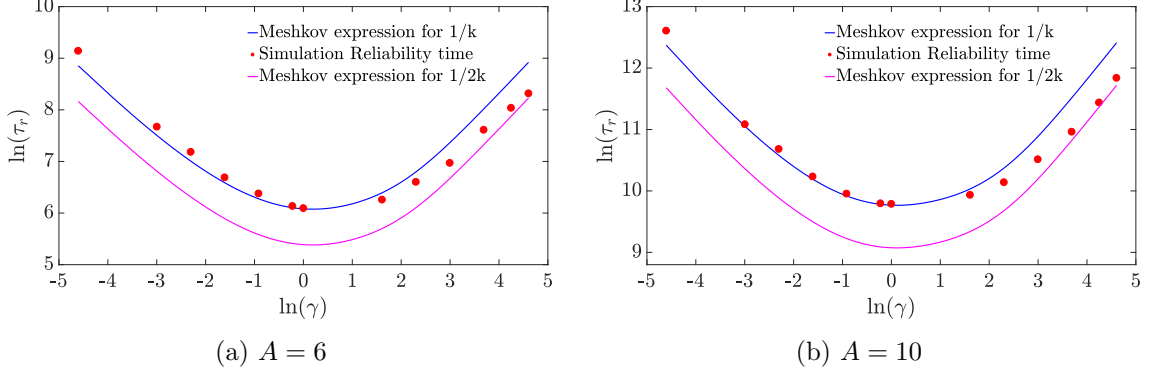


FIGURE 4: The reliability time $\tau_r \propto \frac{1}{\gamma}$ in the low friction regime, $\tau_r \propto \gamma$ in the high friction regime and is minimum at moderate friction. Results are compared to the inverse of escape rate from a single well($1/k$), as predicted by Eq. 13. Here, and elsewhere in the manuscript, error bars are omitted when comparable to data points.

3.2 Erasing time

As noted earlier, the erasing time is composed of two parts: the transport time defined in Eq. 10 and the mixing time defined in Eq. 11. We now present analytical estimates of these times and compare them with numerical solutions.

3.2.1 Transport time

We can obtain an analytical estimate of the transport time in low and high friction limits by assuming that a particle starting at $x = B$ moves deterministically under the influence of the potential slope and drag force.

1. **Low friction regime:** The particle travels with a constant acceleration of $\frac{F}{m}$ and the time taken to travel a distance B is $\tau_t \approx \sqrt{2mB/F}$.

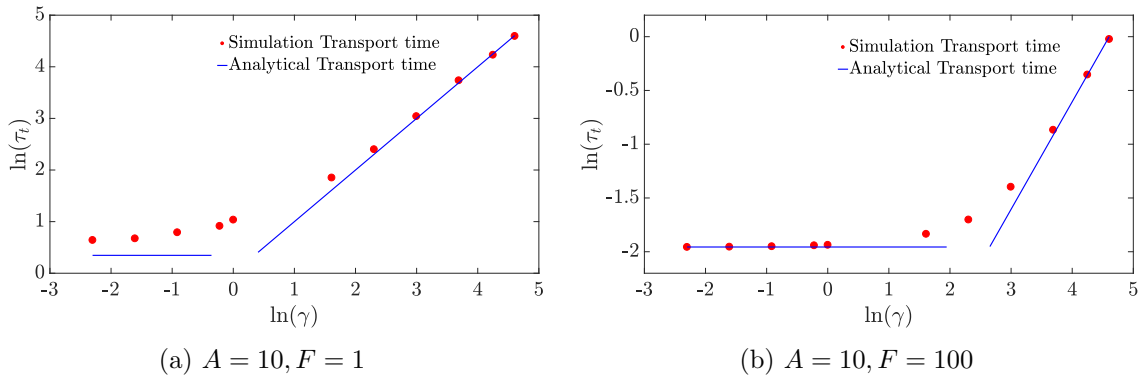


FIGURE 5: The transport time obtained from simulations approximates the analytical estimates of $\tau_t \approx \sqrt{2mB/F}$ in the low friction regime, $\tau_t \approx mB\gamma/F$ ($\propto \gamma$) in the high friction regime.

2. **High friction regime:** In this regime, we assume that the net force on the particle (arising from the sum of drag and potential) is zero. The particle travels with a velocity of $F/m\gamma$, and the time taken to travel a distance B is $\tau_t \approx mB\gamma/F$.

We thus expect the transport time to be constant in the underdamped regime and increase linearly with friction in the overdamped regime. Figure 5 illustrates that this scaling is observed in Langevin simulations, and that numerical values are in reasonable agreement with these crude estimates. The largest quantitative deviations occur at low force and low friction (e.g. $F = 1$ in Figure 5a), when the diffusion of the particle on the slope contributes significantly to τ_t . This results in a simulation transport time larger than the analytical estimate.

3.2.2 Mixing time

Similar to the transport time, analytical estimates of the mixing time can be obtained in the limits of high and low friction.

1. **Low friction regime:** For purposes of approximate calculation we treat the well “0” as a harmonic oscillator. Deterministically, the energy of a harmonic oscillator decays exponentially in the underdamped regime. Therefore we have $E(t) = E_0 e^{-\gamma t}$, where E_0 is the initial energy of the particle when it first reaches $x = 0$ and $E(t)$ is the energy of the particle at time t . In the underdamped regime, a particle starting at B arrives at position $x = 0$ with energy $E_0 \approx A + F \cdot B$. Thus solving for $E(\tau_{\text{mix}}) = A - 3k_B T$,

$$\tau_{\text{mix}} \approx \frac{1}{\gamma} \log \frac{A + F \cdot B}{A - 3k_B T} \quad (14)$$

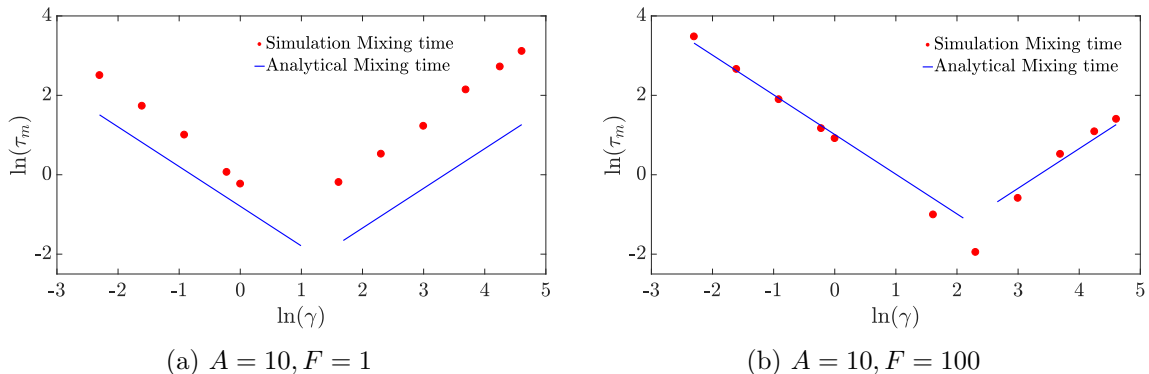


FIGURE 6: Evidence from simulation that the mixing time $\tau_{\text{mix}} \approx \frac{1}{\gamma} \log \frac{A + F \cdot B}{A - 3k_B T} \left(\propto \frac{1}{\gamma} \right)$ in the low friction regime, $\tau_{\text{mix}} \approx \frac{mB^2\gamma}{2\sqrt{2}A} \left(\propto \gamma \right)$ in the high friction regime and is minimised at moderate friction.

2. **High friction regime:** A sensible estimate of the behaviour can be obtained by explicitly modelling the diffusion of the particle near the barrier top. In the overdamped limit, the criterion of reaching a total energy of $E(\tau_{\text{mix}}) = A - 3k_B T$ is equivalent to reaching a point d which has potential energy of $A - 3k_B T$, since momenta are sampled

arbitrarily rapidly in this limit. To proceed, we consider the typical time required to reach an absorbing barrier at d starting from $x = 0$, assuming a sufficiently large F that we can treat $x = 0$ as a reflecting barrier. Starting from the overdamped stochastic differential equation

$$m\gamma dx = -\partial_x U_{A,B}(x) dt + \sqrt{2m\gamma k_B T} dW \quad (15)$$

with generator $\mathcal{L} = \frac{k_B T}{m\gamma} e^{\frac{U_{A,B}(x)}{k_B T}} \partial_x e^{\frac{-U_{A,B}(x)}{k_B T}} \partial_x$, we apply the standard methods outlined in Pavliotis [29, (7.1), pp. 239], which leads to the following system of equations for the average mixing time $\tau_{mix}(x)$ as a function of the initial position x

$$\begin{aligned} \frac{k_B T}{m\gamma} e^{\frac{U_{A,B}(x)}{k_B T}} \partial_x e^{\frac{-U_{A,B}(x)}{k_B T}} \partial_x \tau_{mix}(x) &= -1, \quad d < x \leq 0. \\ \tau_{mix}(x) &= 0, \quad x = d. \end{aligned} \quad (16)$$

We can solve Equation 16 using appropriate limits to get

$$\tau_{mix}(x) = \frac{m\gamma}{k_B T} \int_0^{\sqrt{\frac{3k_B T}{2A}} B} \int_0^q e^{\frac{U(q)-U(r)}{k_B T}} dq dr, \quad (17)$$

where we have approximated the potential near the barrier as an inverted harmonic oscillator to estimate $d = \sqrt{\frac{3k_B T}{2A}} B$. Repeating this approximation within the integral, we obtain

$$\tau_{mix}(x) \approx \frac{m\gamma}{k_B T} \int_0^B \int_0^{\sqrt{\frac{3k_B T}{2A}}} e^{\frac{2A(r^2-q^2)}{B^2 k_B T}} dq dr \approx \frac{mB^2\gamma}{2\sqrt{2A}}. \quad (18)$$

Equations 14 and 18 predict that the mixing time will scale as $1/\gamma$ in the low friction limit and as γ in the high friction limit. In the first case, mixing within the well is limited by the rate at which the particle can reduce its total energy, whereas in the second it is determined by the speed with which the particle can diffuse in position space to a configuration with lower potential energy. We plot simulation results for the mixing time, along with the analytic predictions, in Fig. 6, confirming this scaling and the resultant non-monotonicity. Quantitatively, simulation results deviate from the crude analytic predictions at low force (e.g. $F = 1$ in Figure 6a), when it is no longer reasonable to treat $x = 0$ as either a reflecting barrier or a steep side of a harmonic well. Instead, excursions of the particle back onto the slope occupying the region $x > 0$ lead to much larger mixing times. Nonetheless, the scaling and non-monotonicity in friction are preserved. Combining τ_{trans} and τ_{mix} gives τ_e , plotted in Fig. 7. Analytically, the erasing time is given as:

1. **Low friction regime:**

$$\tau_e \approx \sqrt{\frac{2mB}{F}} + \frac{1}{\gamma} \log \frac{A + F \cdot B}{A - 3k_B T}. \quad (19)$$

2. **High friction regime:**

$$\tau_e \approx \frac{mB\gamma}{F} + \frac{mB^2\gamma}{2\sqrt{2A}} \quad (20)$$

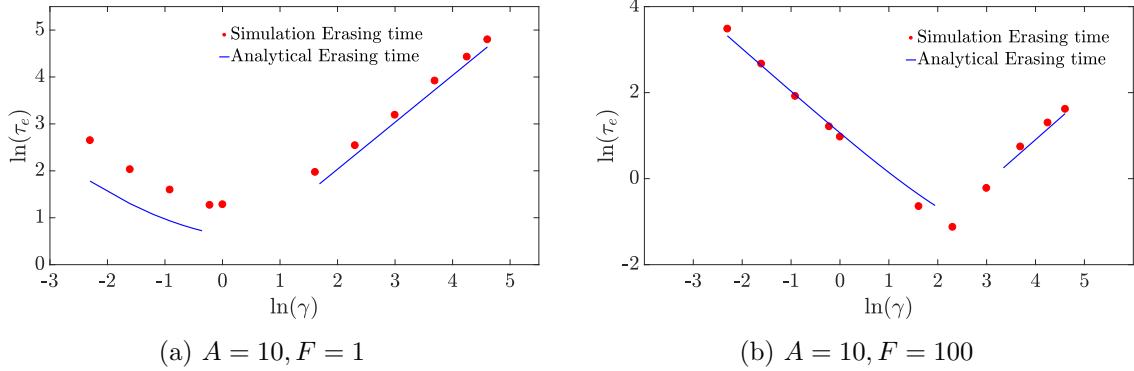


FIGURE 7: Evidence from simulation that the erasing time $\tau_e \approx \sqrt{\frac{2mB}{F}} + \frac{1}{\gamma} \log \frac{A+F\cdot B}{A-3k_B T}$ in the low friction regime, scaling as $1/\gamma$, and $\tau_e \approx \frac{mB\gamma}{F} + \frac{mB^2\gamma}{2\sqrt{2A}}$ in the high friction regime, scaling as γ . The erasing time is minimised at moderate friction.

Like reliability, erasing time is large in the underdamped and overdamped limits, and minimised at intermediate values of friction. The physical cause is the same as before; our erasing protocol involves setting the system into a non-equilibrium state, and waiting for the system to relax towards an equilibrium in the perturbed potential. This process requires the system to diffuse in energy space and also explore configuration space, and is therefore favoured by intermediate friction. Specifically, if the friction is too low, the particle oscillates and slowly loses energy to be confined within the desired well. If the friction is too high, both the transport and mixing times increase as the particle's movement through space is so slow. The relative importance of these effects can be seen in Fig. 8. Once again, this trade-off between high and low friction is not specific to our control, and is likely to be quite generic since any protocol will necessarily push the system out of equilibrium, and will require particles to be typically confined within the target well before the control is removed.

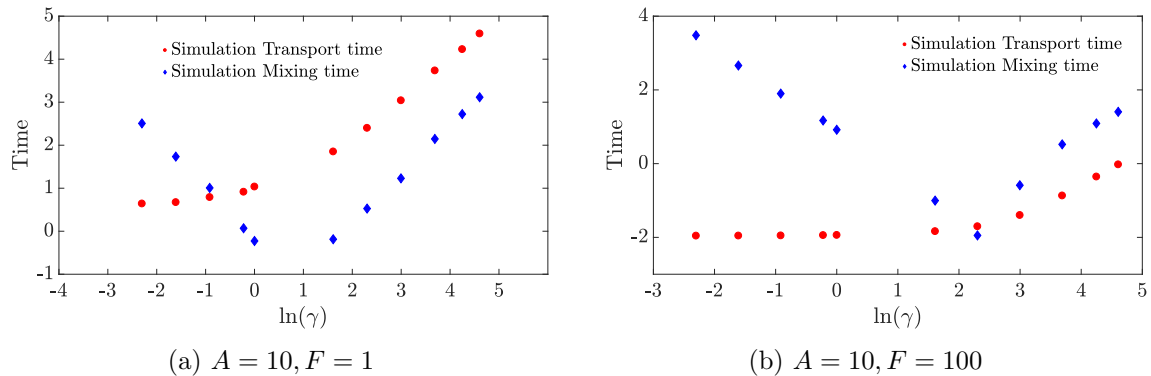


FIGURE 8: Comparison of transport and mixing times. Transport time dominates the mixing time for low force at high friction.

Both erasing and reliability times exhibit a trade-off in friction, being minimised by intermediate values. This fact sets up a second trade-off between designing bits with extreme values of friction to optimise reliability, or moderate values of friction to optimise erasing.

The consequences of this secondary trade-off will be explored in Section 4.

3.2.3 Additional dependencies of the erasing time

A larger value of A implies a steeper descent into the target left-hand well, making mixing faster. We therefore expect that the mixing time and hence the erasing time monotonically decreases with A .

Observation 3.1. The erasing time is a strictly decreasing function of well height A at fixed F, γ . This can be seen from the analytic expressions of erasing time (Equations 19 and 20) backed up with numerical simulations (Figure 9).

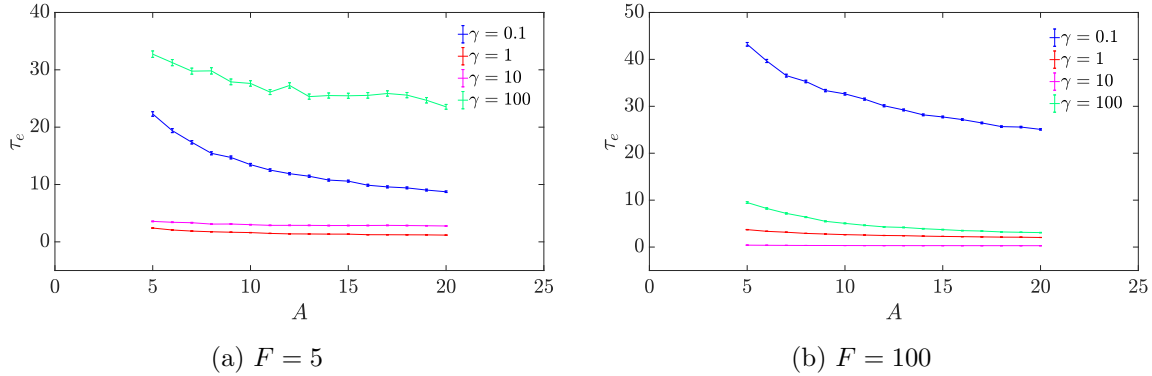


FIGURE 9: Evidence that the erasing time is a strictly decreasing function of well height across a range of F and γ . Other values of F and γ show similar behaviour.

By contrast, erasing time shows a non-monotonic dependence on F at fixed A, γ . Applying too little force leads to slow transport, and doesn't effectively trap the particle within the target well. But applying too much force supplies the particle with too much energy, which must subsequently be lost during the mixing period. The fact that erasing time monotonically decreases with A at fixed F and γ , and shows a non-monotonic dependence on F at fixed A and γ , leads to non-monotonic dependence of τ_e on F at fixed $W = A + F$ and γ . We illustrate this non-monotonicity in Figure 10, in which simple regression formulae have been fitted to the simulation data to enable interpolation at fixed W and γ (see Section C of the Appendix). As friction increases, the force required to provide the particle with excess energy increases, leading to minima at higher values of F .

We make the following observation which will be used in the subsequent section.

Observation 3.2. We have found no evidence of multiple local minima of erasing time in a level set of work for our control family. Physically this fact is unsurprising since the non-monotonicity in τ_e with γ and F mentioned above arise from fairly simple trade-offs, producing curves with single minima.

4 Design of Bits

We are now ready to study the question of how to design good bits. A design involves choosing parameters A, F, γ for a bit to satisfy requirement specifications in terms of speed

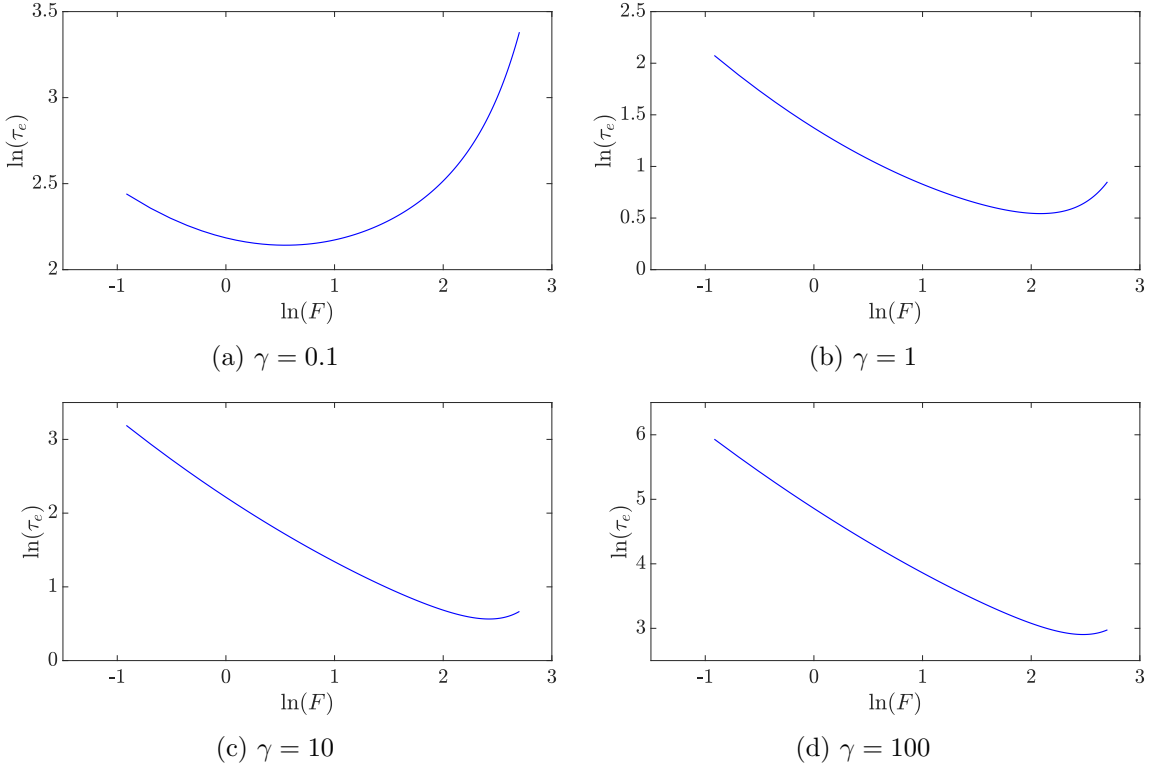


FIGURE 10: For a fixed value of W and γ , the erasing time is a non-monotonic function of F and is minimum at moderate F . This is illustrated at work $W = 20$ for various values of γ .

of erasing and reliability, without expending more work than required. The most general formulation of our problem would require us to also allow the length scale B , the temperature T and the mass m to vary, as well as allowing arbitrary controls. Such a formulation would appear to make the problem even more challenging, so it seems prudent in a first analysis to restrict our analysis to the variables A, F , and γ . Our restricted analysis is not without value since the underlying technology typically does not allow arbitrary variation. Our numerical analysis with Example 2.1 will guide us in our assumptions and analysis, but our results will hold in greater generality. We will construct our proofs based on general assumptions, and subsequently explain how these assumptions are met by our control family.

We introduce the following terms.

1. The design of a bit is completely specified by the **design triple** (A, F, γ) . **Design Space** (\mathcal{DS}) is the space of all design triples (A, F, γ) .
2. A **requirement specification** is a tuple $(t_r, t_e) \in \mathbb{R}_{>0}^2$ denoting the reliability and erasing time we require of the bit. **Requirements Space** (\mathcal{RS}) is the space of all requirement specifications.
3. **Erasing time** $\tau_e : \mathcal{DS} \rightarrow \mathbb{R}_{>0}$ takes a design triple (A, F, γ) to the time required for erasing the corresponding bit under the control protocol specified by F . **Reliability time** $\tau_r : \mathcal{DS} \rightarrow \mathbb{R}_{>0}$ takes a design triple (A, F, γ) to the reliability time of the corre-

sponding bit. Note that τ_r is constant as a function of F since it is a property of the dynamics in the absence of control.

4. **Work** $W : \mathcal{DS} \rightarrow \mathbb{R}_{>0}$ represents the expected work done by the control in erasing the corresponding bit. We will assume that W is constant as a function of γ , as is the case in Example 2.1.
5. A design (A, F, γ) is **feasible** for a requirement (t_r, t_e) iff both $\tau_r(A, F, \gamma) \geq t_r$ and $\tau_e(A, F, \gamma) \leq t_e$. A (t_r, t_e) -feasible design (A, F, γ) is (t_r, t_e) -**optimal** iff the work $W(A, F, \gamma)$ is minimum among all (t_r, t_e) -feasible designs.
6. Inspired by the observation that non-trivial minima of erasing time at fixed work exist for our family of protocols (Section 3.2.3), we define the notion of **trapped** bits. A design (A, F, γ) is **trapped** iff for all designs (A', F', γ') with $W(A, F, \gamma) = W(A', F', \gamma')$, the erasing time $\tau_e(A, F, \gamma) \leq \tau_e(A', F', \gamma')$. A design (A, F, γ) is **uniquely trapped** iff for all designs (A', F', γ') with $W(A, F, \gamma) = W(A', F', \gamma')$, the erasing time $\tau_e(A, F, \gamma) \leq \tau_e(A', F', \gamma')$ with equality iff $(A, F, \gamma) = (A', F', \gamma')$. A design (A, F, γ) is **locally trapped** iff there exists a neighbourhood of (A, F, γ) consisting of bits (A', F', γ') with $W(A, F, \gamma) = W(A', F', \gamma')$ such that the erasing time $\tau_e(A, F, \gamma) \leq \tau_e(A', F', \gamma')$.
7. A requirement specification (t_r, t_e) is **unsaturated** iff there exists a (t_r, t_e) -optimal design (A, F, γ) such that either $\tau_r(A, F, \gamma) > t_r$ or $\tau_e(A, F, \gamma) < t_e$. A feasible requirement specification that is not unsaturated is called **saturated**.

Throughout this section, we will assume that τ_e, τ_r , and W are continuous functions.

The next claim states that an optimal bit always saturates the bound on the erasing time constraint. Further, if the optimal bit is not locally trapped, then it also saturates the bound on the reliability time constraint.

Claim 4.1 (Saturation of timescales). Let us assume that it is possible to locally decrease work at fixed reliability time (This is generally possible since one can perturb the control parameters to reduce work; but reliability time does not depend on the control parameters). Fix requirement specifications $(t_r, t_e) \in \mathcal{RS}$. Suppose (A, F, γ) is a (t_r, t_e) -optimal design. Then

1. $\tau_e(A, F, \gamma) = t_e$.
2. If the design (A, F, γ) is not locally trapped, then $\tau_r(A, F, \gamma) = t_r$.

Proof. 1. For contradiction suppose that $\tau_e(A, F, \gamma) < t_e$. Since τ_e is continuous and it is possible to locally decrease work at fixed reliability time, there exists a design (A', F', γ') with $W(A', F', \gamma') < W(A, F, \gamma)$ that is (t_r, t_e) -feasible contradicting the optimality of the design (A, F, γ) .

2. For contradiction suppose that $\tau_r(A, F, \gamma) > t_r$. Since the design (A, F, γ) is not locally trapped and τ_r is continuous, there exists a design (A_0, F_0, γ_0) requiring work $W(A_0, F_0, \gamma_0) = W(A, F, \gamma)$, erasing time $\tau_e(A_0, F_0, \gamma_0) < \tau_e(A, F, \gamma) \leq t_e$ and maintaining reliability time $\tau_r(A_0, F_0, \gamma_0) \geq t_r$. Thus the design (A_0, F_0, γ_0) is (t_r, t_e) -optimal contradicting claim 4.1. 1 that the optimal design saturates the bound on the erasing time constraint.

□

Observation 4.2. The erasing time of trapped designs is a strictly decreasing function of work for our family of protocols (Example 2.1). In other words, if (A_0, F_0, γ_0) and (A^*, F^*, γ^*) are trapped designs with $W(A^*, F^*, \gamma^*) > W(A_0, F_0, \gamma_0)$ then $\tau_e(A^*, F^*, \gamma^*) < \tau_e(A_0, F_0, \gamma_0)$.

Proof. Since W is a continuous increasing function of A (Observation 2.2), one can choose $A' > A^*$ such that $W(A', F_0, \gamma_0) = W(A^*, F^*, \gamma^*)$. Noting that increasing well height at fixed F and γ decreases erasing time (Observation 3.1), we get $\tau_e(A', F_0, \gamma_0) < \tau_e(A_0, F_0, \gamma_0)$. Using the fact that (A^*, F^*, γ^*) is a trapped design, we get $\tau_e(A^*, F^*, \gamma^*) \leq \tau_e(A', F_0, \gamma_0) < \tau_e(A_0, F_0, \gamma_0)$ establishing the claim. \square

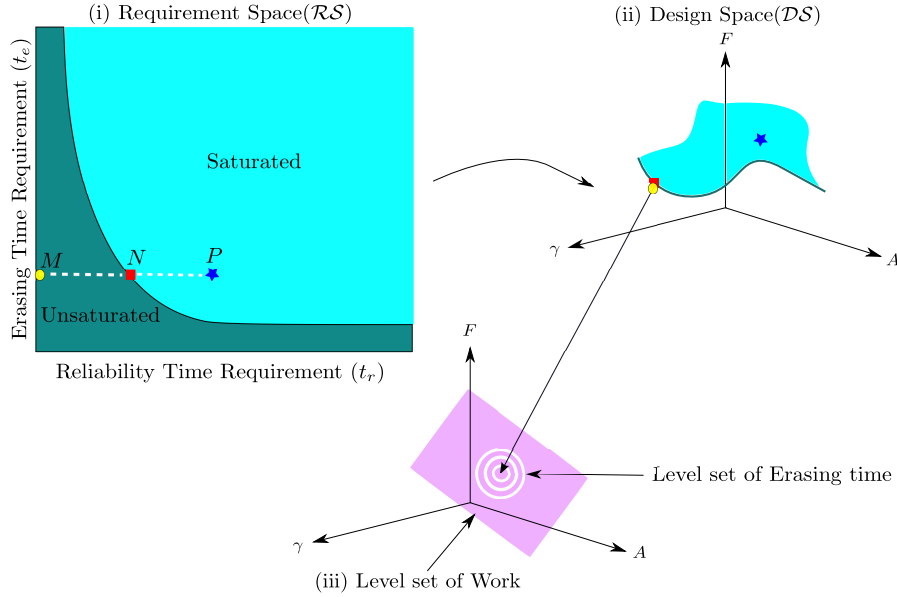


FIGURE 11: An illustration of the mapping of requirement specifications to optimal designs. Points M, N in (i) Requirement Space(\mathcal{RS}) having the same erasing time requirement get mapped to the same optimal bit in (ii) Design Space(\mathcal{DS}). (iii) A representation of a level set of work W within \mathcal{DS} , illustrating that the optimal designs to which unsaturated requirements are mapped minimize erasing time among all designs requiring the same work.

Claim 4.3 (Saturated and Unsaturated Requirements). Assume that the erasing time of trapped designs is a strictly decreasing function of the work (Observation 4.2). Let (A^*, F^*, γ^*) be a trapped design such that $\tau_e(A^*, F^*, \gamma^*) = t_e$.

1. If $t_r \leq \tau_r(A^*, F^*, \gamma^*)$ then (A^*, F^*, γ^*) is (t_r, t_e) -optimal.
2. If $t_r < \tau_r(A^*, F^*, \gamma^*)$ then (t_r, t_e) is unsaturated.
3. Let us make the following assumptions.
 - (a) It is possible to locally decrease work at fixed reliability time.
 - (b) Locally trapped designs are uniquely trapped (as noted for our family of protocols (Example 2.1) in Observation 3.2).

If $t_r \geq \tau_r(A^*, F^*, \gamma^*)$, then (t_r, t_e) is saturated.

Proof. 1. Since $\tau_r(A^*, F^*, \gamma^*) \geq t_r$ and $\tau_e(A^*, F^*, \gamma^*) = t_e$, the design (A^*, F^*, γ^*) is (t_r, t_e) -feasible. Suppose that the design (A^*, F^*, γ^*) is not (t_r, t_e) -optimal. Then there exists a (t_r, t_e) -feasible design (A', F', γ') such that $W(A', F', \gamma') < W(A^*, F^*, \gamma^*)$. Let (A_0, F_0, γ_0) be a trapped design with $W(A_0, F_0, \gamma_0) = W(A', F', \gamma') < W(A^*, F^*, \gamma^*)$. Then $\tau_e(A_0, F_0, \gamma_0) > \tau_e(A^*, F^*, \gamma^*)$ since the erasing time of trapped bits is a strictly decreasing function of work. Using the fact that (A_0, F_0, γ_0) is a trapped design, we get $\tau_e(A', F', \gamma') \geq \tau_e(A_0, F_0, \gamma_0) > \tau_e(A^*, F^*, \gamma^*) = t_e$, a contradiction since (A', F', γ') is a (t_r, t_e) -feasible design.

2. Immediate from claim 4.3. 1.
3. For contradiction suppose that the requirement (t_r, t_e) is unsaturated. Then by claim 4.1. 1 there exists a (t_r, t_e) -optimal design (A_0, F_0, γ_0) such that $\tau_r(A_0, F_0, \gamma_0) > t_r$ and $\tau_e(A_0, F_0, \gamma_0) = \tau_e(A^*, F^*, \gamma^*) = t_e$. Since locally trapped designs are uniquely trapped, using claim 4.1. 2, we get that the design (A_0, F_0, γ_0) must be uniquely trapped. Noting that uniquely trapped bits are trapped and using the fact that the erasing time of trapped designs is a strictly decreasing function of work, we get $W(A_0, F_0, \gamma_0) = W(A^*, F^*, \gamma^*)$. This implies that $(A_0, F_0, \gamma_0) = (A^*, F^*, \gamma^*)$, a contradiction since $\tau_r(A_0, F_0, \gamma_0) > t_r \geq \tau_r(A^*, F^*, \gamma^*)$.

□

The claims about saturation/unsaturation of times-scales can also be proved using KKT conditions (Refer Section E in the Appendix), a standard tool from optimization theory. A more intuitive picture of the results can be understood from Figure 11. In this figure, we illustrate how finding an optimal design subject to a specification maps a point in the requirement space to a point in the design space. For a trapped design (A^*, F^*, γ^*) , requirements with $t_r < \tau_r(A^*, F^*, \gamma^*)$ and $t_e = \tau_e(A^*, F^*, \gamma^*)$ are unsaturated and get mapped to the same design (A^*, F^*, γ^*) (claims 4.3. 2 and 4.3. 1). If the design (A^*, F^*, γ^*) is uniquely trapped, then requirements with $t_r \geq \tau_r(A^*, F^*, \gamma^*)$ and $t_e = \tau_e(A^*, F^*, \gamma^*)$ are saturated (claim 4.3. 3).

Figure 12 illustrates these results for our example family of controls (Example 2.1). As discussed in Section C of the Appendix, we have implemented simple regression to fit the functions $\tau_e(\cdot)$ and $\tau_r(\cdot)$ to our simulation results. We then identified trapped designs using numerical minimisation, plotting the requirement specifications saturated by these designs. For each trapped bit (A^*, F^*, γ^*) , we randomly selected requirements with $t_e = \tau_e(A^*, F^*, \gamma^*)$, but with t_r either greater than or less than $\tau_r(A^*, F^*, \gamma^*)$, and used numerical optimization techniques to search for the optimal designs. The results support our analysis; requirements with $t_r < \tau_r(A^*, F^*, \gamma^*)$ are unsaturated, and those with $t_r \geq \tau_r(A^*, F^*, \gamma^*)$ are saturated. Furthermore, as we show in Figure 12 (b), unsaturated requirements at fixed t_e all map to the same trapped design.

4.1 Optimal Friction for simple controls

In Section 3, we demonstrated that both reliability and erasing times are non-monotonic in friction, with short erasing times favoured by moderate values of friction, and long reliability times favoured by extreme values. In what follows, we give a precise quantification of this trade-off in the setting of optimal bits. The analysis is significantly simplified for our family

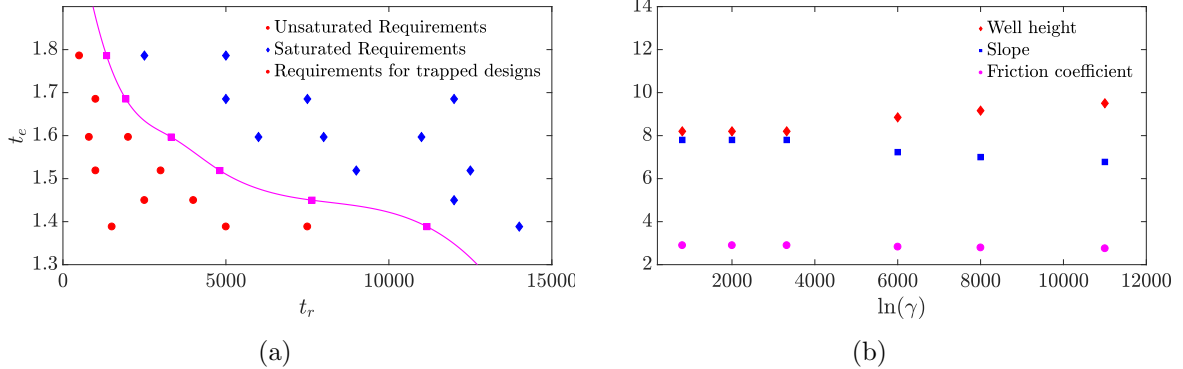


FIGURE 12: Illustration of the division of Requirement Space(\mathcal{RS}) into saturated and unsaturated regions by requirements that correspond to trapped designs. (a) Squares show requirements (t_e, t_r) that are saturated by trapped designs for the family of protocols we consider. Numerical optimization shows that requirements to the left of the locus defined by these points are unsaturated (circles), whereas requirements to the right are saturated (diamonds). (b) A plot of the optimal designs for points from (a) at $t_e = 1.5968$. It is clear that for requirements $t_r \leq 3320.9$, lying to the left of the trapped-design locus in (a), optimal design parameters are identical whereas they are distinct for $t_r > 3320.9$.

of controls, in which work is independent of the friction coefficient.

Let us introduce the following terms. Fix an A and F . Then,

1. γ_{crit}^e is the friction coefficient that minimizes erasing time as a function of friction coefficient γ at fixed A and F , i.e., for all $\gamma' \in \mathbb{R}_{>0}$, we have:

$$\tau_e(A, F, \gamma_{\text{crit}}^e) \leq \tau_e(A, F, \gamma'). \quad (21)$$

We call the design $(A, F, \gamma_{\text{crit}}^e)$ **critically damped**.

2. γ_{crit}^r is the friction coefficient that minimizes reliability time as a function of friction coefficient γ at fixed A and F , i.e., for all $\gamma' \in \mathbb{R}_{>0}$, we have:

$$\tau_r(A, F, \gamma_{\text{crit}}^r) \leq \tau_r(A, F, \gamma'). \quad (22)$$

It is easy to note that trapped bits are also critically damped. In Figure 13 we show illustrative curves of the erasing and reliability times as a function of friction coefficient γ at fixed A, F . These curves have single minima at γ_{crit}^e and γ_{crit}^r , respectively. Also shown on this graphs are regions of friction space that can be eliminated from consideration for optimal bits. To eliminate extreme values of friction, we note that the design must have a minimal finite A to be a well-defined two-state system in the resting state. For our bit, it is $A_{\min} \approx 3$. The next claim makes this precise.

Claim 4.4. [Forbidden regions for optimal friction] Let (A, F, γ) be a (t_r, t_e) -optimal design. (Refer to Figure 13 for notational convenience)

1. Let γ_0 be such that $\tau_r(A, F, \gamma_0) = \tau_r(A, F, \gamma_{\text{crit}}^e)$.

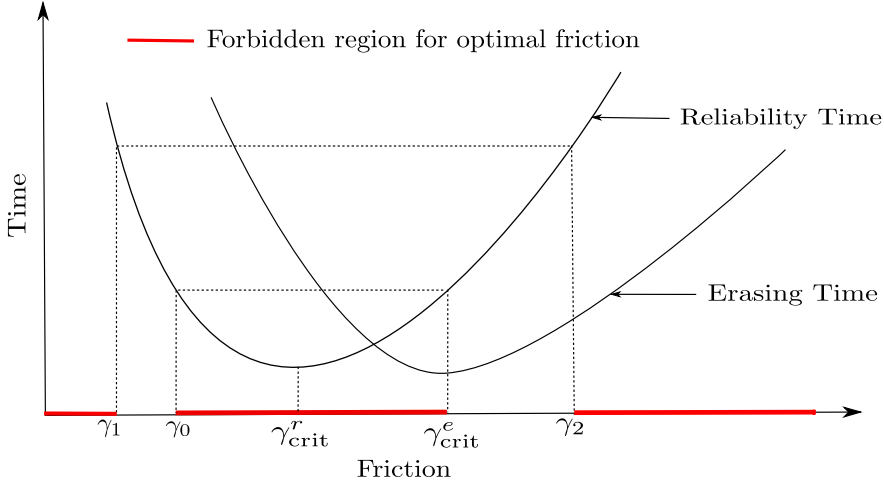


FIGURE 13: Regions of friction-space can be eliminated from the search for optimal bits for our class of controls. As a result, the optimal friction is either critical damping, or lies somewhere within two regions of moderate friction. Illustrative curves of τ_e and τ_r at fixed A, F indicate these regions.

- (a) If $\gamma_{\text{crit}}^e > \gamma_{\text{crit}}^r$, then $\gamma \notin (\gamma_0, \gamma_{\text{crit}}^e)$.
- (b) If $\gamma_{\text{crit}}^e < \gamma_{\text{crit}}^r$, then $\gamma \notin (\gamma_{\text{crit}}^e, \gamma_0)$.
- 2. Let A_{\min} be the minimum height for a bit to be meaningfully bistable and let $\gamma_1 < \gamma_2$ be such that $\tau_r(A_{\min}, F, \gamma_1) = \tau_r(A_{\min}, F, \gamma_2) = t_r$. If (A, F, γ) is not locally trapped, then $\gamma \notin (0, \gamma_1) \cup (\gamma_2, \infty)$.

Proof. 1. We prove it for the case when $\gamma_{\text{crit}}^e > \gamma_{\text{crit}}^r$, the other case proceeds in identical fashion. For contradiction, assume that $\gamma \in (\gamma_0, \gamma_{\text{crit}}^e)$. Then, due to single minima in both τ_e and τ_r , and the fact that τ_e tends to infinity as γ tends to zero or infinity, there exists a design (A, F, γ') with $\gamma' > \gamma_0$ and $\tau_r(A, F, \gamma') = \tau_r(A, F, \gamma) \geq t_r$, but $\tau_e(A, F, \gamma') < \tau_e(A, F, \gamma) \leq t_e$. The design (A, F, γ') is (t_r, t_e) -optimal since it is (t_r, t_e) -feasible and has $W(A, F, \gamma') = W(A, F, \gamma)$, contradicting Lemma 4.1. 1 that the optimal bit saturates the bound on the erasing time constraint.

- 2. For contradiction, suppose that $\gamma < \gamma_1$ or $\gamma > \gamma_2$. Then since $A \geq A_{\min}$ and the reliability time increases with well height and more extreme values of γ , either $\tau_r(A, F, \gamma) \geq \tau_r(A_{\min}, F, \gamma) > \tau_r(A_{\min}, F, \gamma_1) = t_r$ or $\tau_r(A, F, \gamma) \geq \tau_r(A_{\min}, F, \gamma) > \tau_r(A_{\min}, F, \gamma_2) = t_r$, contradicting claim 4.1. 2 that an optimal design that is not locally trapped saturates the bound on the reliability time constraint.

□

Let us assume initially that $\gamma_{\text{crit}}^e > \gamma_{\text{crit}}^r$. We see that optimal designs reside either at γ_{crit}^e , or lie within two regions at moderate friction, as illustrated in Figure 13. Interestingly, one region is adjacent to γ_{crit}^e , whereas the other is not. It is not easy to see how designs in one region ($\gamma_1 \leq \gamma \leq \gamma_0$) as in Figure 13 can outperform those in the other region ($\gamma_{\text{crit}}^e < \gamma \leq \gamma_2$). Indeed, when we performed numerical optimisation on the regression-based

fits to our simulation data, we only observed optimal bits that are critically damped or lie in the allowed region adjacent to critical damping. This is illustrated in Figure 14, where we plot the optimal friction as a function of erasing time requirement at fixed reliability time requirement, for two values of reliability time requirements. We also plot γ_{crit}^e and γ_{crit}^r for comparison. At low erasing time requirements, designs reside at γ_{crit}^e . At slightly higher erasing time requirements, the designs become saturated and the optimal friction lies adjacent to γ_{crit}^e in the region $\gamma_{\text{crit}}^e < \gamma \leq \gamma_2$. Eventually, γ_{crit}^e crosses γ_{crit}^r . At the crossing point, we have $\gamma = \gamma_{\text{crit}}^e = \gamma_{\text{crit}}^r$. At higher values of erasing time requirements, γ still occupies the region adjacent to γ_{crit}^e , which is now $\gamma_1 \leq \gamma \leq \gamma_{\text{crit}}^e < \gamma_{\text{crit}}^r$.

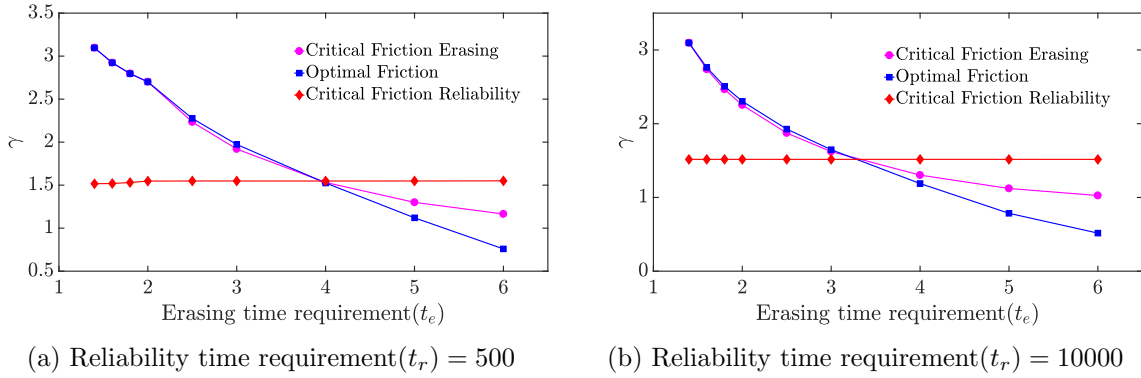


FIGURE 14: Optimal friction is either critical damping, or lies within a small region adjacent to critical damping for our family of controls. We plot friction for optimal designs (A, F, γ) against erasing time requirements(t_e) for a fixed value of reliability time requirement(t_r), alongside γ_{crit}^e and γ_{crit}^r . Note that A and F are not fixed, but determined by the optimisation procedure alongside the optimal friction for each requirement (t_r, t_e) . The data was obtained from numerical optimisation and minimisation based on regression fits to simulation data.

5 Conclusions

We have explored the question of the design of optimal bits. Previously, authors have focused on designing optimal protocols that minimize work input when implementing a finite-time operation on a given system [40, 45, 4, 49, 13]. Our approach differs in considering that bits need to have two distinct functionalities: retain data for long periods of time and allow rapid switching or erasing. Moreover we consider optimising over system parameters such as the intrinsic friction and the external control. Our fundamental observation is that friction plays a non-trivial role in the design of bits. Both switching/erasing and the eventual degradation of data involve relaxation towards equilibrium from a non-equilibrium distribution. This process is fastest at intermediate values of the friction, but slow in the overdamped and underdamped regimes. The best bit designs have high reliability times and low switching/erasing times, which implies an inherent trade-off in bit design between extreme values of friction that favour high reliability, and moderate values of friction that favour rapid switching or erasing.

We have explored the consequences of the biphasic role of friction for a simple class of controls. The existence of non-trivial minima of erasing time in the level set of work leads to the generation of trapped designs. These designs are optimal for reliability requirements

smaller than their own reliability time leading to unsaturated requirements. The result of the trade-off between extreme values of friction that maximize reliability time and moderate values of friction that minimise erasing times is that optimal designs are either critically damped or occupy a region of moderate friction close to critical damping.

Our work opens up a new perspective on the design of efficient computational devices showing that: *the best designs are likely to be neither underdamped nor overdamped*. This observation is particularly important as some authors have considered friction to be inherently problematic for computation [2, 11, 20, 25]. Equally, the role of friction is suppressed when bits are modelled as discrete two-state systems [24, 28, 15], since this approximation assumes rapid equilibration within the discrete states.

Although we have frequently considered a simple family of control protocols in deriving these results, many of them hold for a much broader class. The non-monotonic role of friction in both the erasing and reliability time-scales is a generic physical phenomenon that extends beyond the details of our implementation. Relatively weak assumptions – that it is always possible to decrease work at fixed reliability time and that the minimal erasing time decreases with increased work imply that erasing time requirements are always saturated by optimal bits and that trapped designs lead to unsaturated reliability time requirements respectively. Other results rely more on the simplicity of the control family: the existence of only one local minimum of erasing time at fixed work simplifies the question of whether a requirement specification is saturated. The fact that work is independent of friction simplifies the task of eliminating certain values of friction as sub-optimal.

Allowing a broader class of controls, including those with more complex variation over time, and varying parameters such as particle mass and distance between wells are promising directions for future work. In particular, raising or lowering the barrier between metastable states is a common idea [28, 49, 9, 19]. Lowering the barrier during erasing potentially allows for faster erasing at fixed reliability time and lower work cost. However, in any physical implementation there will be a limit to the extent to which a barrier can be lowered/raised. The considerations presented here will then be relevant to a protocol with optimal barrier manipulation.

Although many of our qualitative findings are likely to be robust, optimizing over more parameters may result in multiple local minima of erasing time at fixed work or the coupling of work to friction, for example. Further, it is not immediately clear whether minima in erasing time at fixed work cost will become more or less prominent features of the optimisation landscape when the complexity of the system is increased. An alternative direction would be to consider similar effects in systems with inherently quantum mechanical behaviour.

6 Competing interests

The authors declare no competing interests.

7 Authors' contributions

MG conceived the project. AD performed the calculations. AD, MG, TEO and NSJ planned the research, analysed the results and wrote the paper.

8 Acknowledgement

We would like to acknowledge Grigoris Pavliotis, Jure Vogrinc, Leonard Adleman, Rahul Dandekar, Tridib Sadhu, Girish Varma, Sanjoy Mitter, Charles Bennett, Deepak Dhar, Vivek Borkar, Venkat Anantharam, David Soloveichik and Aditya Raghavan for useful discussions.

9 Funding

AD is supported by the ROTH scholarship of the Department of Mathematics, Imperial College London. TEO is funded by a University Research Fellowship from the Royal Society.

References

- [1] D. Abreu and U. Seifert, *Thermodynamics of Genuine Nonequilibrium States under Feedback Control*, Physical Review Letters **108** (2012), 030601.
- [2] W. Anacker, *Josephson Computer Technology: An IBM Research Project*, IBM Journal of Research and Development **24** (1980), no. 2, 107–112.
- [3] S. Arrhenius, *Über die Dissociationswärme und den Einfluss der Temperatur auf den Dissociationsgrad der Elektrolyte*, Wilhelm Engelmann, 1889.
- [4] E. Aurell, C. Mejía-Monasterio, and P. Muratore-Ginanneschi, *Optimal Protocols and Optimal Transport in Stochastic Thermodynamics*, Physical Review Letters **106** (2011), 250601.
- [5] A. C. Barato, D. Hartich, and U. Seifert, *Efficiency of cellular information processing*, New Journal of Physics **16** (2014), no. 10, 103024.
- [6] C. H. Bennett, *The thermodynamics of computation—a review*, International Journal of Theoretical Physics **21** (1982), no. 12, 905–940.
- [7] ———, *Notes on the History of Reversible Computation*, IBM Journal of Research and Development **32** (1988), no. 1, 16–23.
- [8] ———, *Notes on Landauer’s principle, reversible computation, and Maxwell’s Demon*, Studies in the History and Philosophy of Modern Physics **34** (2003), 501–510.
- [9] A. Bérut, A. Arakelyan, A. Petrosyan, S. Ciliberto, R. Dillenschneider, and E. Lutz, *Experimental verification of Landauer’s principle linking information and thermodynamics*, Nature **483** (2012), no. 7388, 187–189.
- [10] S. Bo, M. D. Giudice, and A. Celani, *Thermodynamic limits to information harvesting by sensory systems*, Journal of Statistical Mechanics: Theory and Experiment **2015** (2015), no. 1, P01014.
- [11] M. Büttiker, E. P. Harris, and R. Landauer, *Thermal activation in extremely under-damped Josephson-junction circuits*, Physical Review B **28** (1983), 1268–1275.
- [12] M. P. Frank, *The Physical Limits of Computing*, Computing in Science and Engineering **4** (2002), no. 3, 16–26.

- [13] T. R. Gingrich, G. M. Rotskoff, G. E. Crooks, and P. L. Geissler, *Near-optimal protocols in complex nonequilibrium transformations*, Proceedings of the National Academy of Sciences **113** (2016), no. 37, 10263–10268.
- [14] M. Gopalkrishnan, *The Hot Bit I: The Szilard-Landauer Correspondence*, arXiv:1311.3533 [cs.IT] (2013).
- [15] ———, *A Cost/Speed/Reliability Tradeoff to Erasing*, Entropy **18** (2016), no. 5.
- [16] C. C. Govern and P. R. ten Wolde, *Optimal resource allocation in cellular sensing systems*, Proceedings of the National Academy of Sciences **111** (2014), no. 49, 17486–17491.
- [17] P. Hänggi, P. Talkner, and M. Borkovec, *Reaction-rate theory: Fifty years after Kramers*, Reviews of Modern Physics **62** (1990), 251–341.
- [18] J. M. Horowitz and S. Vaikuntanathan, *Nonequilibrium detailed fluctuation theorem for repeated discrete feedback*, Physical Review E **82** (2010), 061120.
- [19] Y. Jun, M. Gavrilov, and J. Bechhoefer, *High-Precision Test of Landauer’s Principle in a Feedback Trap*, Physical Review Letters **113** (2014), 190601.
- [20] M. Klein and A. Mukherjee, *Thermal noise induced switching of Josephson logic devices*, Applied Physics Letters **40** (1982), no. 8, 744–747.
- [21] P. E. Kloeden and E. Platen, *Higher-order implicit strong numerical schemes for stochastic differential equations*, Journal of Statistical Physics **66** (1992), no. 1, 283–314.
- [22] H.A. Kramers, *Brownian motion in a field of force and the diffusion model of chemical reactions*, Physica **7** (1940), no. 4, 284 – 304.
- [23] G. Lan, P. Sartori, S. Neumann, V. Sourjik, and Y. Tu, *The energy-speed-accuracy trade-off in sensory adaptation*, Nature Physics **8** (2012), no. 5, 422–428.
- [24] R. Landauer, *Irreversibility and Heat Generation in the Computing Process*, IBM Journal of Research and Development **5** (1961), no. 3, 183–191.
- [25] K. K. Likharev, *Classical and quantum limitations on energy consumption in computation*, International Journal of Theoretical Physics **21** (1982), no. 3, 311–326.
- [26] J. C. Mattingly and A. M. Stuart, *Geometric ergodicity of some hypo-elliptic diffusions for particle motions*, Markov Processes and Related Fields **8** (2002), no. 2, 199–214.
- [27] V. I. Melnikov and S. V. Meshkov, *Theory of activated rate processes: Exact solution of the Kramers problem*, The Journal of Chemical Physics **85** (1986), no. 2, 1018–1027.
- [28] T. E. Ouldridge, C. C. Govern, and P. R. Wolde, *The thermodynamics of computational copying in biochemical systems*, arXiv:1503.00909 [q-bio.MN] (2015).
- [29] G. A. Pavliotis, *Stochastic processes and applications*, vol. 60, Springer, 2014.
- [30] E. Pollak, H. Grabert, and P. Hänggi, *Theory of activated rate processes for arbitrary frequency dependent friction: Solution of the turnover problem*, The Journal of Chemical Physics **91** (1989), no. 7, 4073–4087.

- [31] M. Ponmurugan, *Generalized detailed fluctuation theorem under nonequilibrium feedback control*, Physical Review E **82** (2010), 031129.
- [32] E. Pop, *Energy dissipation and transport in nanoscale devices*, Nano Research **3** (2010), no. 3, 147–169.
- [33] T. Rapcsák, *Smooth nonlinear optimization in R^n* , Springer **19** (1997), 376.
- [34] B. I. Rapoport, J. T. Kedzierski, and R. Sarpeshkar, *A glucose fuel cell for implantable brain-machine interfaces*, PloS one **7** (2012), no. 6, e38436.
- [35] L. D. Ruslan, H. Richard, and M.V. Tretyakov, *Langevin thermostat for rigid body dynamics*, The Journal of Chemical Physics **130** (2009), no. 23, 234101.
- [36] T. Sagawa and M. Ueda, *Generalized Jarzynski Equality under Nonequilibrium Feedback Control*, Physical Review Letters **104** (2010), 090602.
- [37] _____, *Nonequilibrium thermodynamics of feedback control*, Physical Review E **85** (2012), 021104.
- [38] R. Sarpeshkar, *Analog versus Digital: Extrapolating from Electronics to Neurobiology*, Neural computation **10** (1998), no. 7, 1601–1638.
- [39] _____, *Ultra Low Power Bioelectronics: Fundamentals, Biomedical Applications, and Bio-Inspired Systems*, Cambridge, 002 2010.
- [40] T. Schmiedl and U. Seifert, *Optimal Finite-Time Processes In Stochastic Thermodynamics*, Physical Review Letters **98** (2007), 108301.
- [41] K. Sekimoto, *Kinetic Characterization of Heat Bath and the Energetics of Thermal Ratchet Models*, Journal of the Physical Society of Japan **66** (1997), no. 5, 1234–1237.
- [42] _____, *Langevin Equation and Thermodynamics*, Progress of Theoretical Physics Supplement **130** (1998), 17–27.
- [43] L. Sourabh, R. Shubhashis, and A.M. Jayannavar, *Fluctuation theorems in the presence of information gain and feedback*, Journal of Physics A: Mathematical and Theoretical **45** (2012), no. 6, 065002.
- [44] L. Szilard, *On the decrease of entropy in a thermodynamic system by the intervention of intelligent beings*, Behavioral Science **9** (1964), no. 4, 301–310.
- [45] H. Then and A. Engel, *Computing the optimal protocol for finite-time processes in stochastic thermodynamics*, Physical Review E **77** (2008), 041105.
- [46] Y. Tu, *The nonequilibrium mechanism for ultrasensitivity in a biological switch: Sensing by Maxwell's demons*, Proceedings of the National Academy of Sciences **105** (2008), no. 33, 11737–11741.
- [47] J. L. Vega, R. Guantes, and S. Miret-Artes, *Mean first passage time and the Kramers turnover theory in activated atom-surface diffusion*, Physical Chemistry Chemical Physics **4** (2002), 4985–4991.

[48] S. Wright and J. Nocedal, *Numerical optimization*, Springer Science **35** (1999), 67–68.

[49] P. R. Zulkowski and M. R. DeWeese, *Optimal finite-time erasure of a classical bit*, Physical Review E **89** (2014), 052140.

10 Appendix

A Validating the timestep of the integrator

We validate the accuracy of our Langevin integrator by considering the dependence of thermodynamic expectations on the time step. We calculate the average potential and kinetic energies for a particle in a quadratic potential $W_{A,B} = A \left(\frac{x}{B} - 1 \right)^2$, a quadratic proxy for a single well of the quartic resting-state potential. We plot the results in Figure 15 for a few representative values of the friction coefficient $\gamma = [0.1, 1.10, 100]$ and $A = 10$. Each result is based on an average from 10 simulations each of 5×10^8 time steps. As is evident from the figure, a time step of 0.001 gives good convergence to the equipartition limit of $k_B T/2$.

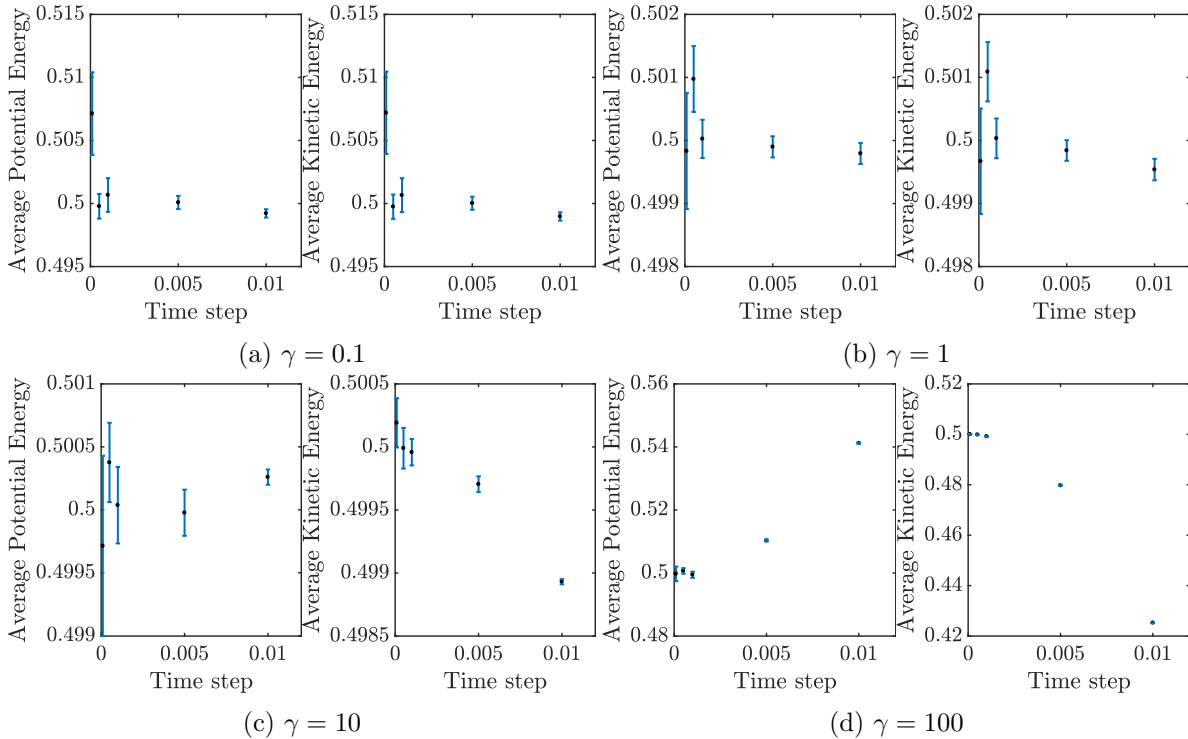


FIGURE 15: A time step of 0.001 is good enough to ensure that the average potential and kinetic energies approaches $\frac{k_B T}{2} = 0.5$ for a wide range of friction values.

However, it is not sufficient to just compare the average kinetic and potential energies to the equipartition limit. We need to ensure that the observed kinetics are robust to our choice of time step. In particular, we need to test that a time step of 0.001 is sufficient for the highest values of our control parameter F , which presents the most severe challenge to integrating our Langevin equation (due to the behaviour near $x = 0$). Figure 16 confirms

that a time step of 0.001 is appropriate for $F = 100$ and the full range of γ tested. Each value in the figure is an average over 1000 initial conditions.

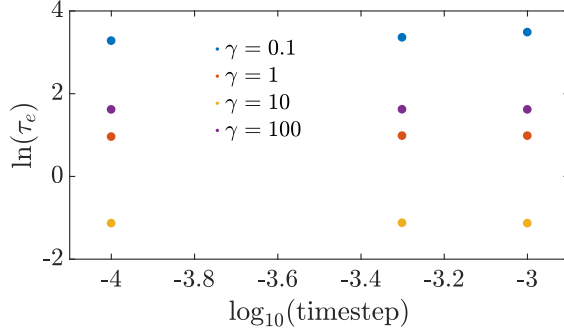


FIGURE 16: A time step of 0.001 gives reasonable values of erasing time for the largest value of the control parameter ($F = 100$) that we use in the simulations.

B Work calculation

B.1 Full calculation for work done at $t=0$

We first provide a more detailed justification of the approximation $W = (A + F \cdot B - k_B T/2)/2$ for the work done when the control potential is switched on, then compare it to the exact result. From Equation 12, and letting $I = \{x \geq 0 \mid A - U_{A,B}(x) + F \cdot x \geq 0\}$, we get

$$\begin{aligned} \langle W \rangle &= \int_0^\tau \int_I V_F(x, t) p(x, t) \delta(t) dx dt \\ &= \int_I (A - U_{A,B}(x) + F \cdot x) p(x, 0) dx \end{aligned} \quad (23)$$

Since $p(x, 0) \propto e^{-\frac{U_{A,B}(x)}{k_B T}}$, we can rewrite the expression of work as

$$\langle W \rangle = \frac{\int_I (A - U_{A,B}(x) + F \cdot x) e^{-\frac{U_{A,B}(x)}{k_B T}} dx}{\int_{-\infty}^{\infty} e^{-\frac{U_{A,B}(x)}{k_B T}} dx} \quad (24)$$

Since $I \subseteq [0, \infty)$ and $(A - U_{A,B}(x) + F \cdot x) e^{-\frac{U_{A,B}(x)}{k_B T}}$ is negligible as $x \rightarrow \infty$, replacing

the upper limit of integration by ∞ is reasonable. Hence the integral becomes

$$\langle W \rangle \approx \frac{\int_0^{\infty} (A - U_{A,B}(x) + F \cdot x) e^{-\frac{U_{A,B}(x)}{k_B T}} dx}{\int_{-\infty}^{\infty} e^{-\frac{U_{A,B}(x)}{k_B T}} dx} \quad (25)$$

When $A \gg k_B T$, we can use Bessel's functions to approximate this integral giving

$$\langle W \rangle \approx \frac{\left(A + F \cdot B - \frac{k_B T}{2} \right)}{2} \quad (26)$$

justifying the crude approximation in the main text.

The accuracy of this expression compared to Eq. 23 is illustrated in Figure 17.

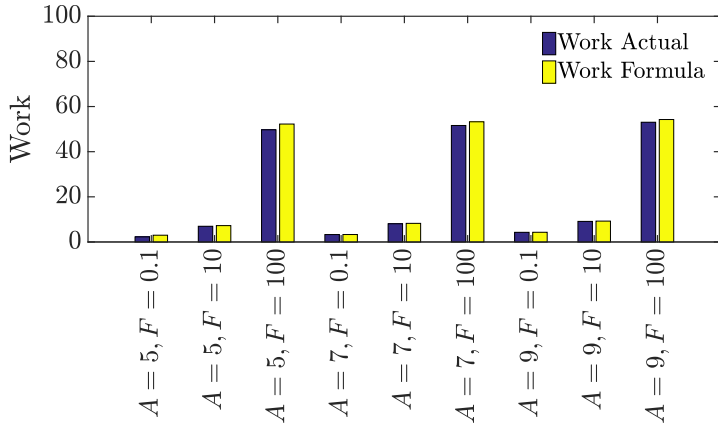


FIGURE 17: Work when the control is switched on against various values of A and F , comparing the full expression Eq. 23 and the approximate result Eq. 26.

B.2 The potential for energy recovery is negligible

Here, we argue that energy recoverable at the end of the protocol is very small, and hence may be neglected. We assume that the control is switched off after a time τ sufficiently large compared to τ_e so that the proportion of particles remaining on the right hand side of the well is determined by the Boltzmann factor. The work that we could then in principle recover is given by the following expression:

$$\langle W_{rec} \rangle \approx \frac{\int_I (A - U_{A,B}(x) + F \cdot x) e^{-\frac{(A+F \cdot x)}{k_B T}} dx}{\int_{-\infty}^0 e^{-\frac{U_{A,B}(x)}{k_B T}} dx + \int_0^{\infty} e^{-\frac{(A+F \cdot x)}{k_B T}} dx} \quad (27)$$

Recall that $I = \{x \geq 0 \mid A - U_{A,B}(x) + F \cdot x \geq 0\}$. This implies that $I = [0, x^*]$, where $A - U_{A,B}(x^*) + F \cdot x^* = 0$. Using Equations 26 and 27, we will calculate the fraction of

recovered work i.e., $W_{rec}^f = \frac{\langle W_{rec} \rangle}{\langle W \rangle}$. Figure 18 precisely calculates this quantity. As is evident from the figure, the fraction is almost negligible and reaches its maximum value at low A and F .

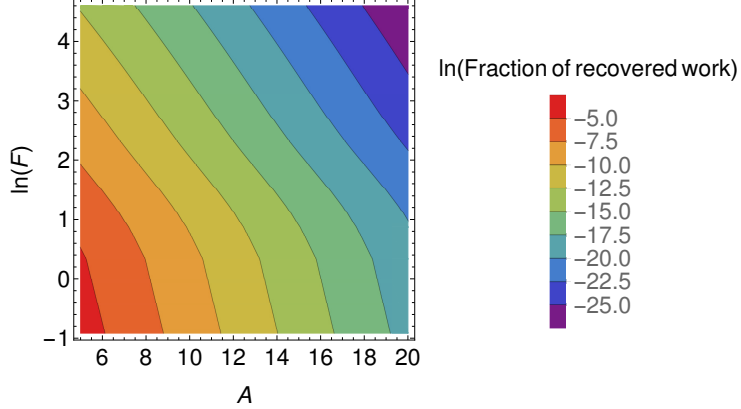


FIGURE 18: Negligible energy can be recovered for our family of controls.

C Regression and Cross Validation

We use cubic regression to interpolate between simulation data for both the reliability and erasing time-scales. Let $F' = \log(F)$ and $\gamma' = \log(\gamma)$. Then we use the following polynomials to fit the time-scales.

1. Erasing Polynomial:

$$\log(\tau_e) = b_1 + b_2 A^3 + b_3 F'^3 + b_4 \gamma'^3 + b_5 A^2 F' + b_6 A' F'^2 + b_7 F'^2 \gamma' + b_8 F' \gamma'^2 \quad (28)$$

$$+ b_9 A'^2 \gamma' + b_{10} A \gamma'^2 + b_{11} A^2 + b_{12} F'^2 + b_{13} \gamma'^2 + b_{14} A F' + b_{15} F' \gamma' \quad (29)$$

$$+ b_{16} A \gamma' + b_{17} A + b_{18} F' + b_{19} \gamma' \quad (30)$$

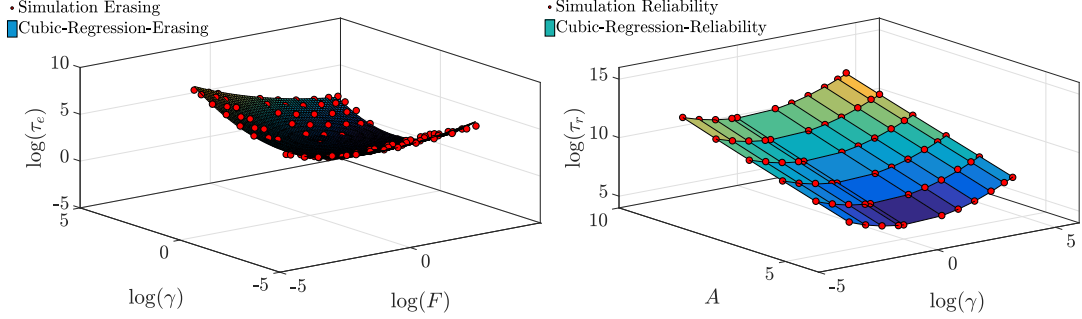
2. Reliability Polynomial:

$$\log(\tau_r) = c_1 + c_2 A^3 + c_3 \gamma'^3 + c_4 A^2 \gamma' + c_5 A \gamma'^2 + c_6 A^2 + c_7 \gamma'^2 + c_8 A \gamma' + c_9 A + c_{10} \gamma \quad (31)$$

, where the coefficients b_1, b_2, \dots, b_{19} and c_1, c_2, \dots, c_{10} are to be determined by regression.

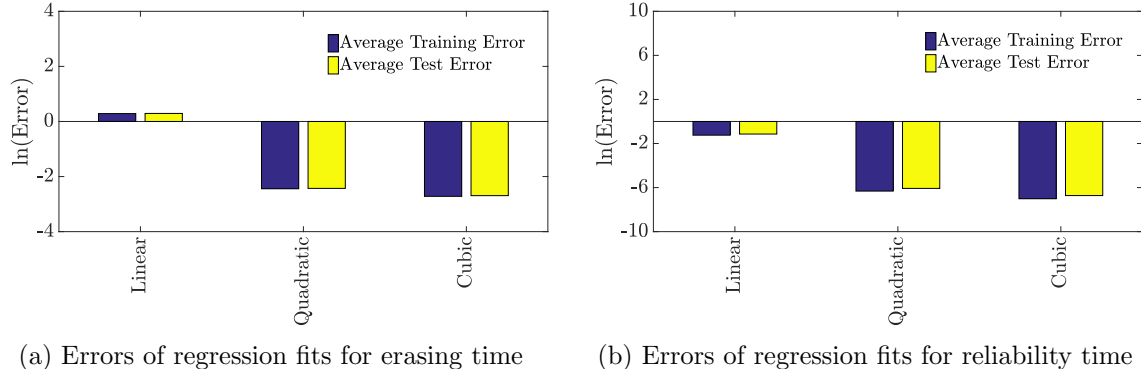
Figure 19 gives a visual illustration of the fact that cubic fits offer a good approximation to the simulation results for both the erasing and reliability time-scales. In what follows, we present a more detailed and formal justification using cross-validation.

We perform “Leave-one-out” cross validation to justify the use of cubic regression. Figure 20 reports the mean square training and testing cross-validation errors corresponding to linear, quadratic and cubic fits. A lower value of the testing error indicates a good fit. Cubic regression has the lowest value of testing errors amongst the fits considered for both the reliability and erasing time-scales. Figure 20 confirms that the training and testing errors corresponding to cubic-regression for both the time-scales are roughly comparable (with



(a) Erasing time from simulation and cubic-regression for $A = 6$ (b) Reliability time from simulation and cubic-regression

FIGURE 19



(a) Errors of regression fits for erasing time (b) Errors of regression fits for reliability time

FIGURE 20

the training error being slightly lower than the testing error). As a result, we can safely assume that the cubic polynomial does not over-fit the data and use it for modelling both the time-scales.

D Calculation of well parameters

Here we calculate the quantities needed to apply Equation 13 to our system, with the potential $U_{A,B}(x) = A \left(\frac{x^2}{B^2} - 1 \right)^2$. We have $\partial_x U_{A,B}(x) = \frac{4Ax(x^2 - B^2)}{B^4}$ and $\partial_{xx} U_{A,B}(x) = \frac{4A(3x^2 - B^2)}{B^4}$.

1. **Angular frequency at barrier height (ω_b):** We can approximate the region near the barrier by an inverted harmonic oscillator. By Taylor expanding the potential about the point $x = 0$, we get

$$U_{A,B}(x) \approx U(0) + \partial_x U_{A,B}(x) \Big|_{x=0} x + \frac{\partial_{xx} U_{A,B}(x) \Big|_{x=0}}{2} x^2 \approx A - \frac{2Ax^2}{B^2} = A - \frac{m\omega_b^2 x^2}{2} \quad (32)$$

Therefore we have $\omega_b = \sqrt{\frac{4A}{mB^2}}$.

2. **Angular frequency at the bottom of the well (ω_0)**: We can approximate the region near the bottom of the well by a harmonic oscillator. By Taylor expanding the potential about the point $x = B$, we get

$$\begin{aligned} U_{A,B}(x) &\approx U(B) + \partial_x U_{A,B}(x) \Big|_{x=B} (x - B) + \frac{\partial_{xx} U_{A,B}(x) \Big|_{x=B} (x - B)^2}{2} \\ &= \frac{4A(x - B)^2}{B^2} = \frac{m\omega_0^2(x - B)^2}{2} \end{aligned} \quad (33)$$

Therefore we have $\omega_0 = \sqrt{\frac{8A}{mB^2}}$.

3. **Action at barrier height $I(A)$** : Consider a particle of mass m with a starting velocity $v = 0$, moving along a constant energy surface with energy A . The particle starts at $x = 0$ and moves to $x = \sqrt{2}B$ and returns back to $x = 0$. The action for this round trip is given by $I(A) = \oint pdx = 2\sqrt{2m} \int_0^{\sqrt{2}B} \sqrt{A - A \left(\frac{x^2}{B^2} - 1 \right)^2} dx = \frac{8B\sqrt{mA}}{3}$.

E KKT conditions

KKT conditions form the foundation of optimization problems [48, 33]. In order to study the KKT conditions, we consider the optimization problem of finding the design with the lowest work that is (t_r, t_e) -feasible.

Problem E.1.

$$\begin{aligned} (A^*, F^*, \gamma^*) &= \arg \inf_{A, F, \gamma} W(A, F) \\ t_r - \tau_r(A^*, \gamma^*) &\leq 0 \\ \tau_e(A^*, F^*, \gamma^*) - t_e &\leq 0 \end{aligned}$$

In order to state the KKT conditions, we will need the notion of a regular point. The following definition will make this precise.

Definition E.2 (Regular point). Let $Sat(x^*)$ denote the set of gradients of the constraints that are saturated at the point x^* . Then x^* is regular iff $Sat(x^*)$ does not form a linearly dependent set.

Theorem E.3 (KKT conditions). Let x^* be a local optimum of E.1 and a regular point. Then by [48, (12.1), pp. 95], there exists $\lambda_1^*, \lambda_2^* \in \mathbb{R}_{\geq 0}$ such that

1. $\nabla W(A^*, F^*, \gamma^*) - \lambda_1^* \nabla \tau_r(A^*, \gamma^*) + \lambda_2^* \nabla \tau_e(A^*, F^*, \gamma^*) = 0$.
2. $\lambda_1^*(t_r - \tau_r(A^*, \gamma^*)) = 0$ and $\lambda_2^*(\tau_e(A^*, F^*, \gamma^*) - t_e) = 0$.

Given this powerful theorem E.3, we are now ready to prove the the same result that we obtained earlier but with the machinery of KKT conditions.

Lemma E.4. Let us assume that it is always possible to locally decrease work at fixed reliability time. Let (A^*, F^*, γ^*) be a local optimum of E.1. Then either

1. The design (A^*, F^*, γ^*) saturates the bound on both constraints i.e. $\tau_r(A^*, \gamma^*) = t_r$ and $\tau_e(A^*, F^*, \gamma^*) = t_e$ or
2. The design (A^*, F^*, γ^*) saturates the bound on the erasing time constraint i.e. $\tau_e(A^*, F^*, \gamma^*) = t_e$ but does not saturate the bound on the reliability time constraint i.e. $\tau_r(A^*, \gamma^*) > t_r$ and is locally trapped.

Proof. Consider an optimal design (A^*, F^*, γ^*) such that either it does not saturate the bound on the reliability time constraint i.e. $\tau_r(A^*, \gamma^*) > t_r$ or it does not saturate the bound on the erasing time constraint i.e. $\tau_e(A^*, F^*, \gamma^*) < t_e$. Then we have the following cases:

- Case 1: The design (A^*, F^*, γ^*) saturates the bound on the erasing time constraint, but does not saturate the bound on the reliability time constraint i.e. $\tau_r(A^*, \gamma^*) > t_r$ and $\tau_e(A^*, F^*, \gamma^*) = t_e$. This implies that $\lambda_1^* = 0$. Since only one constraint is active, (A^*, F^*, γ^*) is a regular point. Hence, by Theorem E.3 on KKT conditions, there exists $\lambda_2^* > 0$ such that $\nabla W(A^*, F^*, \gamma^*) + \lambda_2^* \nabla \tau_e(A^*, F^*, \gamma^*) = 0$. This implies that (A^*, F^*, γ^*) is a stationary point of erasing time in the level set of it's work $W(A^*, F^*, \gamma^*)$. The fact that this stationary point is actually a local minimum follows from claim 4.1. 2.
- Case 2: The design (A^*, F^*, γ^*) saturates the bound on the reliability time constraint, but does not saturate the bound on the erasing time constraint i.e. $\tau_r(A^*, \gamma^*) = t_r$ and $\tau_e(A^*, F^*, \gamma^*) < t_e$. This implies that $\lambda_2^* = 0$. Since only one constraint is active, (A^*, F^*, γ^*) is a regular point. Hence, by Theorem E.3 on KKT conditions, there exists $\lambda_1^* > 0$ such that $\nabla W(A^*, F^*, \gamma^*) = \lambda_1^* \nabla \tau_r(A^*, \gamma^*)$, a contradiction since $\frac{\partial W}{\partial F} \neq 0$ but $\frac{\partial \tau_r}{\partial F} = 0$.
- Case 3: The design (A^*, F^*, γ^*) does not saturate the bound on either constraints i.e. $\tau_r(A^*, \gamma^*) > t_r$ and $\tau_e(A^*, F^*, \gamma^*) < t_e$. Since no constraint is active we have $\nabla W(A^*, F^*, \gamma^*) = 0$, which is not possible.

□